Diffraction of Mössbauer gamma rays in crystals

V. A. Belyakov

All-Union Scientific Institute of Physical-Technical and Radio-Technical Measurements, Mendeleevo (Moscow Region)

Usp. Fiz. Nauk **115**, 553–601 (April 1975)

The article is the first review in the world's literature of research on diffraction of Mössbauer γ rays in crystals. This field of research has developed recently and independently, and has involved both experimental and theoretical studies. Its development is due, on the one hand, to the unique possibilities provided by Mössbauer radiation for investigation of the nature of a number of phenomena of solid-state physics and nuclear physics and, on the other hand, to the alluring promise of use of Mössbauer radiation diffraction in applications. The review discusses the current state of research and the most important directions of the studies. These include studies, important in investigation of crystal structure, on determination of the phase of the x-ray structure factor, on the structure of magnetic and electric fields in crystals, on separation of coherent elastic and inelastic scattering of γ rays in crystals, and on coherent Coulomb excitation of low-lying nuclear levels. The research described is promising in applications and shows that a new diffraction method is in the process of being established—Mössbauerography, which has a number of interesting possibilities and is a useful addition to traditional diffraction methods of research such as x-ray and neutron diffraction. The phenomenon of suppression of the inelastic channels of nuclear reactions in Mössbauer diffraction is discussed in detail. Most of the article is devoted to exposition of the theory of the phenomena mentioned and to the specific properties of Mössbauer coherent scattering which distinguish it from diffraction of other types of radiation in crystals.

PACS numbers: 76.80.

CONTENTS

1. INTRODUCTION

As a result of the extraordinarily wide application of the Mössbauer effect in very diverse areas of pure and applied physics, it is appropriate at the present time to discuss not the Mössbauer effect in general, as was done during the first years after discovery of the effect,[1] but its use in some particular area of research (see for example ref. 2). One of these areas, which has developed recently, is the diffraction of Mössbauer radiation in its resonance scattering in crystals. Study of the diffraction of Mössbauer radiation (Mössbauer diffraction) presents significant interest for various reasons. In the first place, its use in structure research is extremely promising. A special term, Mössbauerography[13], already exists for the technique of structure research based on Mössbauer diffraction. The differences of Mössbauer diffraction from the diffraction of x rays, neutrons, and electrons permit information on crystals to be obtained by its use which would be very difficult or practically impossible to obtain by other diffraction techniques. We have in mind here first of all the possibility of determining the phase of the structure factor. The knowledge of this phase is necessary in a structure analysis for the unique deciphering of the structure of a compound. However, its determination is an extremely difficult problem when traditional diffraction methods are used, especially in the case of complex compounds.

The Mössbauer method of determining the structure factor phase is based on an extremely simple method of varying the phase and amplitude of resonance scattering of a γ ray by Mössbauer nucleus by removing the nuclear scattering from the conditions of exact resonance by means of the Doppler effect. Here the amplitude of the Rayleigh scattering (scattering by electrons) remains unchanged. Measuring experimentally the modulus of the combined Rayleigh and nuclear amplitude for three values of Doppler energy shift, it is possible, by using the known dependence on energy of the nuclear resonance amplitude, to calculate the phase of the Rayleigh amplitude.

Mössbauer diffraction also permits investigation of the magnetic structure of a crystal, and it can form the basis for a method of determining directly the magnetic structure of crystals, which is a useful addition to the only method available at the present time for direct investigation of the magnetic structure, magnetic neutronography. The physical basis for the possibility of studying magnetic structure by means of Mössbauer diffraction is the dependence of the Mössbauer scattering amplitude on the direction of the magnetic field at the scattering nucleus, which as we know is due to the orientation of the atomic moment. The dependence of the Mössbauer scattering amplitude on the electric field gradient at the nucleus presents the possibility of investigating by means of Mössbauer diffraction the structure of the electric field gradients in the crystal. For example, it would be possible to establish the different orientation of the electric field gradient tensor axes at equivalent sites of the crystal unit cell.

Another direction of research is the study of the collective interaction of the nuclei of the crystal with γ radiation. As a result of the existence of this interaction in scattering by the crystal when the Bragg condition is

satisfied, the resonance value of γ-ray energy and the energy width of the resonance turn out to be different from the energy and width of the Mössbauer level of an isolated nucleus. Another manifestation of the collective nature of the interaction of γ rays with the nuclei is the suppression of the inelastic channels of nuclear reactions. This effect appears in the fact that, on incidence on a perfect crystal at the Bragg angle, γ rays penetrate through a thickness of crystal substantially greater than the thickness of the same material which the radiation can penetrate in the case of imperfect crystals or of perfect crystals when the Bragg condition is not satisfied. This phenomenon is a nuclear analog of the Borrmann effect, which is well known in x-ray diffraction.

Finally, Mössbauer diffraction is of definite interest theoretically. This is due to the fact that the existing theory of diffraction of various forms of radiation in crystals, particularly the dynamical theory, is limited mainly to discussion of cases in which the scattering amplitude of an individual atom is of the simplest form. That is, the theory utilizes the amplitude for scattering by a scalar center, taking into account if necessary the anisotropy of thermal lattice vibrations by means of the Debye-Waller factor. Experiments on Mössbauer diffraction of γ rays in crystals require for their quantitative description a development of the theory for the case of a more complicated form of the amplitude for scattering by an individual center.

Thus, experimental studies of Mössbauer diffraction, on the one hand, stimulate the detailed development of a theory taking into account the nonscalar nature of the individual scattering centers and, on the other hand, provide the possibility of experimental verification of the conclusions of this theory. The difference between these conclusions and the well known theoretical results for the case of scalar scattering centers lies mainly in the polarization properties of the radiation in the crystal and the experimentally observable effects associated with them in diffraction experiments.

In what we have said above, it has been important that in the crystal scattering the γ rays there are Mössbauer nuclei in which resonance γ-ray scattering occurs. There is also interest in the case of scattering of Mössbauer radiation by crystals not containing a Mössbauer isotope. At first glance it would appear that in this case the diffraction of the γ rays will occur in completely the same way as x-ray diffraction and that it will not be possible to obtain by this means any new information on the crystal beyond that obtainable by means of x rays. However, use of the Mössbauer method for detection of the scattered radiation permits obtaining information inaccessible by the x-ray method. By utilizing the exceptionally high energy resolution of Mössbauer detectors, it is easily possible to separate the elastic and diffuse scattering in the region of the diffraction peak. This permits study of the dynamics of the crystal lattice, observing, for example, the variation with temperature of the fraction of elastically scattered photons.

The first experiments on Mössbauer diffraction were carried out by Moon, Black, and their co-workers of the Birmingham group.[3,4] The goal of the first experiments, which used polycrystalline scatters, was to demonstrate the coherence of nuclear elastic scattering. The question of experimental verification of the coherence of nuclear scattering was raised for the following reason. The time of nuclear resonance scattering, which is determined by the lifetime of the Mössbauer level, is in a typical case 10^{-7}–10^{-8} sec, i.e., significantly greater than the reciprocal frequencies of excitations in a solid. Therefore the preservation of phase relations in scattering of a γ ray by the different nuclei of the crystal for such large scattering times is a very interesting possibility which is not completely obvious and which deserves experimental verification. The coherence of nuclear resonance scattering was demonstrated experimentally in the experiments of Moon, Black, and co-workers in interference of Rayleigh and nuclear scattering in the diffraction peak, which appeared as an asymmetric dependence of the scattering intensity on the Mössbauer source velocity (Fig. 1).

The theoretical problem of coherence of nuclear and Rayleigh scattering has been considered by Moon,[5] Tsara,[6] and Lipkin.[7] Bernstein and Campbell[8] investigated the effect of nuclear scattering on the critical reflection of γ rays from the enriched iron isotope Fe^{57}.

Soon after publication of the first experimental work of the Birmingham group[3], a number of theoretical articles[9-13] suggested use of Mössbauer radiation for diffraction studies, including determination of the phase of the structure factor. For most Mössbauer transitions the wavelength of the γ radiation is $\lambda \sim 10^{-8}$ cm, i.e., in a range convenient for diffraction experiments. So far no experimental determinations of phases have been carried out by this method for compounds with an unknown structure, but recently Mössbauer and co-workers[14,15] have demonstrated with a known structure the practical achievability of determining the structure factor phase by this method.

The first successful experiments on Mössbauer diffraction in single crystals[16-19] stimulated further development of the theory.[20-29] Kagan and Afanas'ev[22-26] developed the dynamical theory of Mössbauer diffraction and investigated in detail the suppression of nuclear-reaction inelastic channels, the so-called Kagan-Afanas'ev effect. The independent work of Hannon and Trammell[28,29] was devoted also to derivation of the general equations of the dynamical theory. Voĭtovetskiĭ[30-35] and Sklyarevskiĭ[36-39] and their co-workers observed the Kagan-Afans'ev effect and studied it experimentally. A gener-

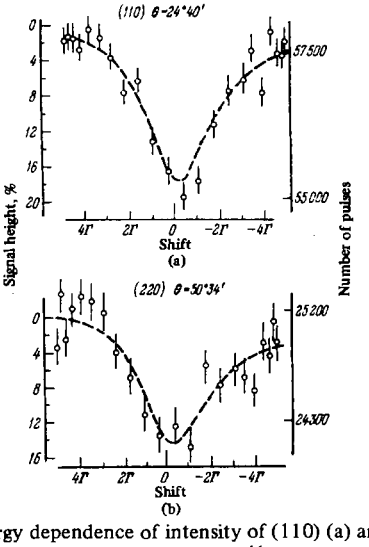

FIG. 1. Energy dependence of intensity of (110) (a) and (220) (b) diffraction peaks for an iron single crystal. [16]

alization of the results of the first studies of Mössbauer diffraction and the suppression effect has been published by Kagan and Afanas'ev.[40]

As was noted above, the dependence of the Mössbauer amplitude on magnetic field and on the electric field gradient[41-44] opens the possibility of using Mössbauer diffraction in structure studies inaccessible by x-ray diffraction and associated with the order of magnetic and electric fields in crystals. In the kinematic approximation the corresponding theory for the simplest cases has been developed by Aĭvazyan and the author.[42, 45-48] In particular, the existence has been noted in Mössbauer scattering of magnetic[47] and quadrupole[48] diffraction peaks which are absent in Rayleigh scattering of γ rays. In subsequent work of the same group[49, 50] the kinematic theory of Mössbauer diffraction has been developed for all the main types of magnetic order in crystals. In the experimental work of the Sklyarevskiĭ group, magnetic[51] and quadrupole[52] diffraction peaks in Mössbauer scattering were observed for the first time. The same group[39, 53] has begun study of the line shape in the nuclear (magnetic) diffraction peak and its dependence on the order of reflection and the departure of the nuclear scattering from exact resonance conditions. Here a number of interesting results have already been obtained which have not yet found complete theoretical interpretation.

Considerable interest is presented by work on the Mössbauer optics of crystals.[54-62] In the presence of resonance interaction of γ rays with nuclei, the optical characteristics of a crystal for γ radiation depend substantially on this interaction. In the case of hyperfine magnetic or quadrupole splitting of the Mössbauer line in the crystal, the crystal will exhibit double refraction and optical activity. The relative strength of these effects turns out to be substantially greater than in the case of the same effects for the optical region. As in ordinary optics, these phenomena can be used to obtain information on the magnetic[56-60] and crystalline[61] structure of the crystal. We will refer those interested in the optics of Mössbauer radiation to the original literature,[54-62] and will limit ourselves to discussion only of questions of the the diffraction of Mössbauer radiation.

2. AMPLITUDE OF COHERENT MÖSSBAUER SCATTERING

a) Introductory remarks. Mössbauer radiation consists of γ rays whose energy typically lies in the range from several to a hundred or more keV and whose wavelength correspondingly lies in the range from several angstroms to several tenths of an angstrom. This means that the energies and wavelengths of Mössbauer radiation are just in the region of energies and wavelengths usually used in x-ray diffraction. Why then, in spite of of the fact that x rays and Mössbauer γ rays are electromagnetic radiation in the same range of wavelengths, is their scattering in crystals of a completely different nature? A general answer to this question is as follows. The cause of the difference is the uniquely low energy width of the Mössbauer radiation, Γ, whose value is typically 10^{-8} eV (we recall that the corresponding value for characteristic x rays is of the order of 1 eV). As a consequence, in diffraction of Mössbauer radiation in crystals, in addition to the same scattering of γ rays by atomic electrons as occurs for x rays, their resonance scattering by nuclei turns out to be very important. In addition, nuclear scattering for Mössbauer γ rays often is dominant, while for x rays it is completely unimportant. As a result, we have a qualitative difference in scattering of these two types of radiation by crystals.

b) Elastic scattering amplitude. For quantitative description of Mössbauer diffraction, it is necessary to dwell in more detail on the features of the elementary event of resonance γ-ray scattering. Let us therefore discuss first the amplitude for elastic scattering of a resonance γ ray by an individual Mössbauer atom of a crystal. The scattering amplitude f is the sum of two terms, a nuclear resonance term f^N and an electronic (Rayleigh) term f^R:

$$f(\mathbf{k}, \mathbf{e}; \mathbf{k}', \mathbf{e}') = f^N(\mathbf{k}, \mathbf{e}; \mathbf{k}', \mathbf{e}') + f^R(\mathbf{k}, \mathbf{e}; \mathbf{k}', \mathbf{e}'), \qquad (2.1)$$

where $\mathbf{k}$, $\mathbf{e}$ and $\mathbf{k}'$, $\mathbf{e}'$ are the wave vector and polarization vector of the γ ray before and after scattering, respectively. The amplitude f^R is identical to the amplitude for scattering of x rays and has the well known form[63]: $f^R(\mathbf{k}, \mathbf{e}; \mathbf{k}', \mathbf{e}') = Zr_e\mathbf{e}'^*\mathbf{e}$, where Z is the number of electrons in the atom and r_e is the classical electron radius. As already noted, nuclear resonance scattering involves all of the specific properties of Mössbauer diffraction, and therefore we will discuss in more detail the amplitude f^N. In view of the large lifetime of Mössbauer levels (the characteristic value of this lifetime is of the order 10^{-7} sec) the resonance elastic-scattering process can be divided into two stages:

1) Resonance γ-ray absorption, transferring the nucleus to the Mössbauer (excited) level; 2) emission without recoil by the excited nucleus of a γ ray, which returns the nucleus to the ground state.

Therefore the scattering cross section turns out to be proportional to the product of the probability of γ-ray absorption without recoil and the probability of emission without recoil, and contains a resonance dependence on the scattered γ-ray energy E. Since in the general case the nucleus in the crystal is subjected to the action of electric and magnetic fields and its levels are split, the resonance energies in the scattering are the energy differences of the sublevels of the excited and ground states. Accordingly, the amplitude for resonance Mössbauer scattering of a γ ray through a definite sublevel m of the ground state and a sublevel m′ of the excited state of the nucleus (for definiteness we will assume that a magnetic field $\mathbf{H}$ acts on the nucleus, and m and m′ are the projections of the spins of the ground and excited states of the nucleus on the direction of the field) can be written in the form[50]

$$f^N_{mm'} = \frac{\pi}{k}\Gamma_{mm'} f(\mathbf{k}) f(\mathbf{k}') \frac{(\mathbf{e}\mathbf{n}^*_{mm'}(\mathbf{k}))(\mathbf{n}_{mm'}(\mathbf{k}')\mathbf{e}'^*)\sqrt{I^{mm'}(\mathbf{k})\, I^{mm'}(\mathbf{k}')}}{E - E_{mm'} + (i\Gamma/2)}, \qquad (2.2)$$

where

$$\Gamma_{mm'} = (2j'+1)\begin{pmatrix} j & L & j' \\ m & M & -m' \end{pmatrix}\Gamma_i$$

is the partial radiation width of the transition from level m′ to level m, Γ and Γ_i are the total and radiation widths of the Mössbauer level[64], L is the transition multipolarity (here and everywhere below where it does not result in confusion we will omit the indices j and j′ designating the spins of the ground state and excited state of the nucleus), $I^{mm'}(\mathbf{k})$ and $\mathbf{n}_{mm'}(\mathbf{k})$ are the normalized intensity ($\int I^{mm'}(\mathbf{k})\, d\Omega_{\mathbf{k}} = 1$ and polarization vector of the radiation emitted in a direction $\mathbf{k}$ in the transition m′ → m, $E_{mm'}$ is the energy difference of levels m′ and m, and $f^2(\mathbf{k})$ is the Lamb-Mössbauer fac-

tor for emission and absorption of a γ ray in direction k. General formulas for $I^{mm'}(\mathbf{k})$ and $\mathbf{n}_{mm'}(\mathbf{k})$ for nuclear transitions of pure and mixed multipolarity have been given in refs. 46, 65, and 66. Here we will write out the expressions for these quantities in the case of dipole and quadrupole transitions of pure multipolarity,

$$I^M(\mathbf{k}) = \frac{1}{4\pi}[e_1^2(M\mathbf{k}) + e_2^2(M\mathbf{k})], \tag{2.3}$$

$$\mathbf{n}_M(\mathbf{k}) = (\chi_2 \cos\alpha_M + i\sin\alpha_M\chi_1)\, e^{iM\varphi}, \tag{2.4}$$

$$\chi_2 = \frac{[\mathbf{k}[\mathbf{H}\mathbf{k}]]}{|[\mathbf{H}\mathbf{k}]|}, \quad \chi_1 = \frac{[\mathbf{H}\mathbf{k}]}{|[\mathbf{H}\mathbf{k}]|}, \quad \operatorname{tg}\alpha_M = \frac{e_2(M\mathbf{k})}{e_1(M\mathbf{k})}, \tag{2.5}$$

where $M = m' - m$, θ is the angle between k and H, φ is the azimuthal angle of the vector k around H (Fig. 2), and the values of e_1 and e_2 are given in the table.

Note that in the numerator of formula (2.2) the product of the factors depending on the wave vector k is a quantity proportional to the matrix element of absorption by the nucleus in the transition $m \to m'$ of a γ ray with wave vector k and polarization vector e. The similar product of the factors depending on k' is proportional to the matrix element for emission of a γ ray with polarization vector e'. Equation (2.2) describes a resonance state directly if the Zeeman splitting of the nuclear levels is substantially greater than the width Γ of the Mössbauer level. In the general case to obtain the amplitude for resonance scattering for a nucleus in the state m, the expression (2.2) must be summed over the intermediate states m'.

As follows from Eq. (2.2), in the general case in the presence of interaction of a Mössbauer nucleus with a magnetic field or an electric field gradient, the explicit form of dependence of the nuclear amplitude on the scattering angle and polarization of the γ ray can be extremely complex. However, without yet giving this dependence in detail, we can see, for example, from Eq. (2.2) that in the case of scattering by a nucleus in a magnetic field the scattering amplitude depends on the direction of the magnetic field. This is evident already from the fact that the intensities entering into Eq. (2.2) for radiation in the Zeeman transition $I^{mm'}(\mathbf{k})$ depend on the field direction, for example, for a dipole transition, as $I^{mm'} \sim \sin^2\theta$. Below we will consider in more detail this dependence in Zeeman splitting, which significantly exceeds the nuclear level width when the scattering occurs through a completely determined Zeeman level of the excited nucleus and the nuclear amplitude is given directly by expression (2.2).

In the case when e and e' correspond to circular polarization, the amplitude (2.2) is conveniently expressed in terms of the finite-rotation matrix elements $D^{(1)}_{mm'}$. Here Eq. (2.2) takes the form[41, 67]

$$f^N(\mathbf{k}, \mu; \mathbf{k}', \mu') = (\mu\mu')^{L-l+1} \begin{pmatrix} j & L & j' \\ m & M & -m' \end{pmatrix}^2 \frac{f(\mathbf{k})\, f(\mathbf{k}')\, D^{(L)}_{\mu' M}(\mathbf{k}'\mathbf{H})\, D^{*(L)}_{\mu M}(\mathbf{k}\mathbf{H})\, |\chi(L, l)|^2}{E_\gamma - E_{mm'} + (i\Gamma/2)}, \tag{2.6}$$

where $\chi(L, l)$ is the reduced matrix element, and the indices μ and μ' describe the polarization of the primary and scattered waves and take on the two values $+1$ and -1, corresponding to right-handed and left-handed circular polarization. Similarly we can find the dependence of the resonance scattering amplitude on the orientation of the principal axes of the tensor of the electric field gradient acting on the nucleus.[42]

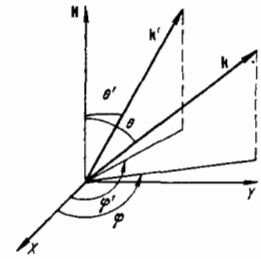

FIG. 2. Definition of angles in expressions for intensity and polarization of γ rays.

c) Isotopic and spin incoherence. The formulas that describe the diffraction of Mössbauer radiation do not involve the amplitude (2.1), but rather the coherent amplitude obtained by averaging (2.1) over the crystal. In the nuclear scattering amplitude there are two factors which lead to incoherence of elastic scattering by the individual atoms of a crystal: 1) isotopic incoherence, and 2) spin incoherence.

Isotopic incoherence is due to the fact that a given isotope of the element considered scatters in a resonant manner, and the presence at a site of another isotope is equivalent to the absence of nuclear scattering in general. Accordingly, the coherent amplitude turns out to be proportional to p, the relative content of the Mössbauer isotope.

Spin incoherence is due to the dependence of the resonance scattering amplitude on the value of m, the projection of the nuclear spin in the ground state. In this case the coherent amplitude is obtained by averaging the expression for the elastic-scattering amplitude over m. Thus, the final expression for the coherent amplitude has the form

$$f^N(\mathbf{k}, \mathbf{e}; \mathbf{k}', \mathbf{e}')_{\text{coh}} = p\sum_m a_m f_m(\mathbf{k}, \mathbf{e}; \mathbf{k}', \mathbf{e}'), \tag{2.7}$$

where a_m is the filling number of a state with nuclear angular momentum projection m, and f_m is determined by Eq. (2.2). The dependence of a_m on m must be taken into account if there is a polarization of the nuclear spin[68] due to cooling of the crystal to temperatures at which an ordering of nuclear spins sets in, or due to special external influences on the crystal. In the case of absence of nuclear polarization, to which we will limit ourselves below, the filling number does not depend on m, and $a_m \equiv (2j+1)^{-1}$.

d) Coherent amplitude in limiting cases of completely split and unsplit lines. The explicit form of the dependence f^N_{coh} on polarization and scattering angle in the general case turns out to be very complicated. These

Values of $e_i^n = \left|\begin{pmatrix} j & L & j' \\ m & M & -m' \end{pmatrix}\right|^{-1} e_l$ for dipole and quadrupole transitions

$e_i^n(M)$	$E(1)$	$M1$	$E2$	$M2$
$e_1^n(0)$	$-\sqrt{\frac{3}{2}}\sin\theta$	0	$\frac{1}{2}\sqrt{\frac{15}{2}}\sin 2\theta$	0
$e_1^n(\pm1)$	$\mp\frac{\sqrt{3}}{2}\cos\theta$	$-\frac{\sqrt{3}}{2}$	$\frac{\sqrt{5}}{2}\cos 2\theta$	$\pm\frac{\sqrt{5}}{2}\cos\theta$
$e_1^n(\pm2)$			$-\frac{\sqrt{5}}{4}\sin 2\theta$	$\mp\frac{\sqrt{5}}{2}\sin\theta$
$e_2^n(0)$	0	$\sqrt{\frac{3}{2}}\sin\theta$	0	$-\frac{1}{2}\sqrt{\frac{15}{2}}\sin 2\theta$
$e_2^n(\pm1)$	$\frac{\sqrt{3}}{2}$	$\pm\frac{\sqrt{3}}{2}\cos\theta$	$\mp\frac{\sqrt{5}}{2}\cos\theta$	$-\frac{\sqrt{5}}{2}\cos 2\theta$
$e_2^n(\pm2)$			$\pm\frac{\sqrt{5}}{2}\sin\theta$	$\frac{\sqrt{5}}{4}\sin 2\theta$

expressions are substantially simplified in the limiting cases of Zeeman splitting which significantly exceeds the Mössbauer level width, and the total absence of Zeeman splitting.

In the first case for a fixed γ-ray energy only one term turns out to be important in Eq. (2.7), that corresponding to resonance scattering through a completely determined Zeeman transition with a coherent amplitude

$$f^N(\mathbf{k}, \mathbf{e}; \mathbf{k}', \mathbf{e}')_{\text{coh}} = \frac{\pi p \Gamma_{mm'} f(\mathbf{k}) f(\mathbf{k}') (\mathbf{e}\mathbf{n}^*_{mm'}(\mathbf{k})) (\mathbf{n}_{mm'}(\mathbf{k}')\mathbf{e}'^*) \sqrt{I(\mathbf{k}) I(\mathbf{k}')}}{k(2j+1)[E_\gamma - E_{mm'} + (i\Gamma/2)]}. \tag{2.8}$$

In the second case, by using Eqs. (2.2) and (2.6), in which the energy denominator now does not depend on m and m′, it is possible to carry out the summation in Eq. (27) in general form. For dipole transitions, for example, the formula for the coherent amplitude takes the form

$$f^N(\mathbf{k}, \mathbf{e}; \mathbf{k}', \mathbf{e}')_{\text{coh}} = \frac{p(2j'+1)\Gamma_i f(\mathbf{k}) f(\mathbf{k}')}{4k(2j+1)[E_\gamma - E_0 + (i\Gamma/2)]} \times \begin{cases} (\mathbf{e}\mathbf{e}'^*), \\ k^{-2}[\mathbf{k}\mathbf{e}][\mathbf{k}'\mathbf{e}'^*], \end{cases} \tag{2.9}$$

where the upper line on the right-hand side refers to electric-dipole transitions, and the lower line to magnetic-dipole transitions. Using Eqs. (2.8) and (2.9), we can easily obtain a representation of the relative values of the coherent-scattering cross section, the γ-ray absorption cross section, and the Rayleigh-scattering cross section. Using the optical theorem $\sigma_T = -(4\pi/k)\,\mathrm{Im}\, f(\mathbf{k}, \mathbf{e}; \mathbf{k}, \mathbf{e})$ we find from (2.9) for the total cross section for absorption by one nucleus σ_T

$$\sigma_T = \frac{p(2j'+1)\pi}{(2j+1)} f^2(\mathbf{k}) \frac{\Gamma\Gamma_i}{2k^2} \left| E_\gamma - E_0 + \frac{i\Gamma}{2} \right|^{-2}. \tag{2.10}$$

The cross section for coherent scattering by one nucleus is:

$$\sigma_{\text{coh}} = \frac{\pi p^2 (2j'+1)^2}{6(2j+1)^2} \frac{f^2(k) f^2(k')}{k^2} \left| \frac{\Gamma_i}{E_\gamma - E_0 + (i\Gamma/2)} \right|^2. \tag{2.11}$$

The radiation width Γ_i is related to Γ by the expression $\Gamma_i = \Gamma(1+\alpha)^{-1}$, where α is the γ-ray internal-conversion coefficient. In order to give an idea of the ratios of the cross sections for coherent nuclear scattering, absorption, and Rayleigh scattering, we will give numerical values obtained from Eqs. (2.9)–(2.10) for an iron crystal. The differential cross section for coherent nuclear scattering is $(d\sigma/d\Omega)_N \sim 3p^2 \cdot 10^3$ barns at the exact resonance. The cross section for coherent rayleigh scattering $(d\sigma/d\Omega)_R$, in contrast to nuclear scattering, depends strongly on angle and is equal to 40 barns for scattering at zero angle and ~4 barns for scattering at 60°. The cross section for nuclear absorption at the resonance is $\sigma_T \sim p \times 10^6$ barns.

We note that, as a result of the fact that nuclear scattering is a slow process in comparison with the inverse frequencies of excitations in the crystal, the thermal factor in the coherent amplitude enters in the form of the product of two Lamb-Mössbauer factors $\exp(-k^2\langle x^2\rangle_{\mathbf{k}}) \exp(-k^2\langle x^2\rangle_{\mathbf{k}'})$ and not in form of the Debye-Waller factor $\exp(-|\mathbf{k}-\mathbf{k}'|\langle x^2\rangle_{\mathbf{k}-\mathbf{k}'})$, as occurs for the coherent-scattering amplitude of x rays ($\langle x^2\rangle_{\mathbf{k}}$ is the mean square of the thermal vibrations in the $\mathbf{k}$ direction). This explains the smooth dependence on scattering angle noted above for nuclear coherent scattering and the rapid drop with increasing angle of the Rayleigh-scattering cross section.

3. KINEMATIC THEORY OF MÖSSBAUER DIFFRACTION

a) Introductory remarks. The main qualitative features of Mössbauer coherent scattering of γ rays in crystals can be described in the kinematic approximation of diffraction theory. This approximation is valid under the conditions of scattering of γ rays in crystals of small size, where the intensity of the scattered beam is much less than that of the primary beam. With small modifications the same approximation is applicable for description of scattering in imperfect (mosaic) crystals of arbitrary size, under the condition that the scattering in an individual crystallite (block) satisfies the requirement formulated above. As in the diffraction of x rays, the principal quantity determining scattering in this case is the structure factor F, which is the sum of the coherent scattering amplitudes (with inclusion of phase factors determined by the location) of all atoms of the unit cell. A special feature of the scattering of Mössbauer radiation is the fact that the structure factor consists of the sum of two terms. One of them, due to scattering of γ rays by electrons, is identical to the well known structure factor for x rays. The other term is due to nuclear scattering and, in contrast to the x-ray structure factor, turns out to depend in a resonant manner on the γ-ray energy and also on the magnitude and structure of the hyperfine fields (electric and magnetic) acting on the Mössbauer nucleus. As a result the cross section for scattering and the polarization of the scattered radiation depend both on the energy of the Mössbauer γ rays and on the magnetic and electric structure of the crystal. Since the x-ray structure factor does not depend on the energy (small energy variations of the γ rays near the resonance value are involved), while the magnitude and phase of the nuclear amplitude depend substantially on energy (see Eq. (2.2)), the scattering cross section as a function of energy has a sharply expressed interference form and can be conveniently represented as the sum of Rayleigh, nuclear, and interference terms. Below we carry out an analysis of the energy and polarization characteristics of Mössbauer coherent scattering in paramagnetic and magnetically ordered crystals in the kinematic approximation.

b) Diffraction in the case of an unsplit Mössbauer line. The differential cross section for scattering of unpolarized radiation per unit cell of the crystal is given by the formula

$$\frac{d\sigma}{d\Omega_{\mathbf{k}'}} = \frac{(2\pi)^3}{V} \overline{|F_\tau|^2}\, \delta(\mathbf{k}-\mathbf{k}'-\tau) = \frac{(2\pi)^3}{V} (\sigma^R_\tau + \sigma^N_\tau + \sigma^{RN}_\tau)\, \delta(\mathbf{k}-\mathbf{k}'-\tau), \tag{3.1a}$$

where V is the volume of the unit cell, τ is the reciprocal lattice vector multiplied by 2π, and $|F_\tau|^2$ is the structure factor averaged over the photon polarization. In the right hand side of Eq. (3.1a) we have separated the total scattering cross section into the Rayleigh cross section σ^R, the nuclear cross section σ^N, and the interference cross section σ^{RN}. It follows from Eq. (3.1a) that diffraction peaks in scattering in a crystal exist only for fulfillment of the relation

$$\mathbf{k} - \mathbf{k}' = \tau \tag{3.1b}$$

–the Bragg condition. The structure factor F_τ is given by the formula

$$F_\tau(\mathbf{k}, \mathbf{e}; \mathbf{k}', \mathbf{e}') = F^R_\tau(\mathbf{k}, \mathbf{e}; \mathbf{k}', \mathbf{e}') + F^N_\tau(\mathbf{k}, \mathbf{e}; \mathbf{k}', \mathbf{e}') = \mathbf{e}\mathbf{e}'^* F^R_\tau + \sum_q f^q(\mathbf{k}, \mathbf{e}; \mathbf{k}', \mathbf{e}')_{\text{coh}} \exp[i(\mathbf{k}-\mathbf{k}')\mathbf{r}_q], \tag{3.2a}$$

where the summation in the last term is carried out only over the Mössbauer nuclei, and F_τ^R is the well known x-ray structure factor. We will consider first the diffraction of Mössbauer radiation in a crystal with an unsplit Mössbauer line. Then the structure factor can be conveniently written for vectors e and e′ corresponding to linear polarization π (lying in the scattering plane) and perpendicular polarization σ (perpendicular to the scattering plane). For these polarizations the structure factor can be represented in the form

$$F_\tau = F_\tau^R P^R + F_\tau^N P^N, \qquad (3.2b)$$

where P^R and P^N are the Rayleigh and nuclear polarization factors, and F_τ^N is defined by Eq. (3.1) if we use in it for f_{coh}^N the expression (2.9), omitting the factor containing the product of the polarization vectors. The form of P^N depends on the multipolarity of the Mössbauer transition. For example, for an E1 transition we have $P^N = P^R$ ($P^R = \cos 2\theta$ for π polarization and $P^R = 1$ for σ polarization, where 2θ is the scattering angle). For an M1 transition, $P^N = 1$ for π polarization and $P^N = \cos 2\theta$ for σ polarization.

A characteristic feature of Mössbauer diffraction in the case considered is interference of the nuclear and Rayleigh scattering. For an unpolarized incident beam the intensity of the scattered radiation in the diffraction peak is determined by the expression

$$\sigma^R + \sigma^N + \sigma^{RN} = |F_\tau^R|^2 \frac{1+\cos^2 2\theta}{2} + \overline{|F_\tau^N P|^2} + 2\,\mathrm{Re}\, F_\tau^N F_\tau^{R*} \overline{P^N P^R}, \qquad (3.3)$$

where the bars over the second and third terms signify polarization averaging. For an E1 nuclear transition the interference term in Eq. (3.3) takes the form $(1+\cos^2 2\theta)\,\mathrm{Re}\, F_\tau^N F_\tau^{R*}$, and for an M1 transition it is $2\cos 2\theta\ \mathrm{Re}\, F_\tau^N F_\tau^{R*}$*. In view of the resonance dependence of the magnitude and phase of the nuclear scattering amplitude on the γ-ray energy, which enters through the factor $[E_\gamma - E + (i\Gamma/2)]^{-1}$, and the constancy of the Rayleigh amplitude for the energy variations considered, the intensity of the scattered radiation as a function of E_γ has a clearly expressed dispersion form. In Fig. 1 we have shown an experimental curve in which interference of the nuclear and Rayleigh scattering is evident.

c) Determination of the phase of the structure factor. The dependence of the modulus and phase of the nuclear amplitude on energy, in combination with the possibility of calculation of these quantities for each γ-ray energy value, permits determination by means of Mössbauer diffraction of the phase of the x-ray structure factor F^R. Particular interest from the point of view of structure studies is presented by Mössbauer determination of the structure-factor phase in the case of complex compounds with a large number of atoms in the unit cell, where determination of this phase by traditional methods is extraordinarily complicated.

The Mössbauer technique for phase determination[10-12] is similar to the method, well known in x-ray structure analysis, of isomorphic substitution and anomalous dispersion[69] and is illustrated in Fig. 3, taken from ref. 15. To determine the phase of the structure factor it is sufficient to make measurements of the intensity in the diffraction peak in the absence of nuclear scattering (for large Doppler shifts of the γ-ray energy) and for two different values of E_γ for which the nuclear scattering amplitude is sufficiently large. The first measurement gives the modulus of the structure factor (in Fig. 3 this

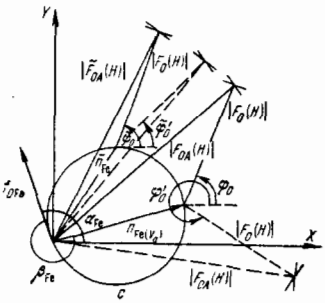

FIG. 3. Principle of determination of the phase φ_0 of the x-ray structure factor [15] $F_0(H)$. $F_{0A}(H)$ and $\tilde{F}_{0A}(H)$ are the total nuclear and Rayleigh scattering amplitudes of the unit cell, and $n_{Fe}(\tilde{n}_{Fe})$ is the nuclear resonance scattering amplitude, which is dependent on the γ-ray energy.

is $|F_0(H)|$), and the last two give the modulus of the sum of the nuclear amplitude and the structure factor (in the figure these are $|F_{0A}(H)|$ and $|\tilde{F}_{0A}(H)|$). Then, by using the calculated value of the nuclear amplitudes n_{Fe} and $\tilde{n}_{Fe}$ for the corresponding energy values, it is possible by means of the geometrical construction shown in Fig. 3 to determine the structure-factor phase φ_0 uniquely.

d) Diffraction in magnetically ordered crystals. If magnetic fields act on the Mössbauer nuclei in a magnetically ordered crystal, the differential cross section for scattering of unpolarized radiation is given by Eq. (3.1a), in which τ is the reciprocal-lattice vector with inclusion of the magnetic structure of the crystal, and the remaining designations are the same as above. The diffraction pattern in this case is similar in its general features to the diffraction of neutrons in magnetically ordered crystals. Therefore the magnetic structure of the crystal can be determined from data on Mössbauer diffraction, exactly as in the case of magnetic neutronography.

While the possibility of determining the phase of the structure factor is quite obvious as a result of the fact that the phase of the nuclear scattering can be changed by means of the Doppler effect, the possibility of determining the magnetic structure of the crystal is not at all obvious at first glance. In fact, in a magnetically ordered crystal, for example, at not too low temperatures there is ordering of the atomic spins, but the nuclear spins are completely unordered (Fig. 4). It therefore seems strange how diffraction of γ rays in a system of unordered nuclei can provide information on the existence of magnetic order in the crystal. The case of very low temperatures, at which ordering of the nuclear spins is achieved, is another matter.[68]

However, this possibility actually exists and is due to the low energy width of the Mössbauer line $\Gamma \sim 10^{-8}$ eV, which leads to a preferential participation in the scattering of nuclei with a definite spin orientation relative to H, and the coherent amplitude turns out to be dependent on H. For example, in the case of complete resolution of the Zeeman splitting, for coincidence of the γ-ray energy with the energy of one of the Zeeman transitions $E_{mm'}$, the scattering occurs essentially only through this one transition. This means that in resonance scattering only nuclei with a spin projection m on the magnetic field direction take part, while nuclei with

FIG. 4. Illustration of the disorder in orientation of nuclear moments (small arrows) in a crystal with ordered atomic moments (heavy arrows).

other values of spin projection play practically no part in the scattering. However, in view of the fact that the nuclear spins are oriented chaotically, on the average only one of 2j + 1 Mössbauer nuclei takes part in the scattering. This leads only to a decrease in the coherent amplitude by a factor 2j + 1 in comparison with the case of complete ordering of the nuclear spins, but the diffraction pattern remains qualitatively the same as for ordered nuclear spins.

Strictly speaking, Mössbauer diffraction provides the possibility of direct determination of the nature of ordering of magnetic fields in Mössbauer nuclei. However, since the nature of the ordering of magnetic fields in nuclei is determined by the ordering of the atomic angular momenta in the crystal, we will discuss the Mössbauer determination of the magnetic structure in the generally accepted meaning of this word. As will be shown below, information on the magnetic structure of the crystal is given not only by the set of observed magnetic maxima and their intensity, but also by the polarization of the radiation in the diffraction peaks. From the discussion of the Mössbauer scattering amplitude given above, it follows that Eq. (3.1) describes both crystalline diffraction peaks determined by the crystalline unit cell of the crystal, and the magnetic peaks determined by the magnetic unit cell. It should be noted that, in view of the extremely weak dependence of the Rayleigh scattering amplitude on orientation of the magnetic moment of the atom[70] (in what follows we will completely neglect it), the magnetic diffraction peaks receive contributions practically only from nuclear scattering and contain no interference of nuclear and Rayleigh scattering. In the crystalline peaks there is a contribution of both Rayleigh and nuclear scattering and therefore the interference of these two forms of scattering appears in them to the full extent.

e) Polarization characteristics of scattering. In this section we will present general expressions relating the polarization characteristics of the scattered radiation with the magnetic structure of the crystal, and also with the polarization, energy, and energy width of the scattered γ-ray line. For this purpose we will write out the differential cross section for scattering of polarized radiation

$$\frac{d\sigma(\mathbf{k}, \mathbf{e}; \mathbf{k}', \mathbf{e}')}{d\Omega_{\mathbf{k}'}} = \frac{(2\pi)^3}{V} |F_{\tau}(\mathbf{k}, \mathbf{e}; \mathbf{k}', \mathbf{e}')|^2 \delta(\mathbf{k} - \mathbf{k}' - \tau), \quad (3.4)$$

where the designations are the same as above. Expression (3.4), as a function of e′ reaches a maximum for some value $\mathbf{e}' \equiv \mathbf{n}_0'$. The vector $\mathbf{n}_0'(\mathbf{e})$ is the polarization vector of the scattered radiation, and the cross section corresponding to it

$$\frac{d\sigma(\mathbf{k}, \mathbf{e}; \mathbf{k}', \mathbf{n}_0')}{d\Omega_{\mathbf{k}'}} \equiv \frac{d\sigma(\mathbf{k}, \mathbf{e}; \mathbf{k}')}{d\Omega_{\mathbf{k}'}}$$

is the differential cross section for scattering of a γ ray with a polarization vector **e**. Introducing the coherent-scattering tensor T_{ik} for the unit cell[63], which is related to the structure factor by the expression

$$F(\mathbf{k}, \mathbf{e}; \mathbf{k}', \mathbf{e}') = \sum_{i,k} e_i'^* T_{ik} e_k \equiv \mathbf{e}'^* \hat{T} \mathbf{e}, \quad (3.5)$$

we obtain the following expression for $\mathbf{n}_0'(\mathbf{e})$:

$$\mathbf{n}_0'(\mathbf{e}) = \hat{T}\mathbf{e} \,|\, \hat{T}\mathbf{e}|^{-1}, \quad (3.6)$$

where the symbol $\hat{T}_{\mathbf{e}}$ indicates a vector whose k-th component is $\sum_i T_{ki} e_i$. We will give an explicit expression for the vector $\mathbf{n}_0'$ below for some special cases. The cross section for scattering of unpolarized radiation is expressed in terms of $d\sigma(\mathbf{ke}; \mathbf{k}')$ by the relation

$$\frac{d\sigma}{d\Omega_{\mathbf{k}'}} = \frac{1}{2} \sum_{i=1,2} \frac{d\sigma(\mathbf{k}, \mathbf{e}_i; \mathbf{k}')}{d\Omega_{\mathbf{k}'}}, \quad (3.7)$$

where the summation is carried out over two mutually orthogonal polarization vectors $\mathbf{e}_i$. The scattered radiation in this case turns out to be partially polarized, and its polarization matrix is

$$\rho = \sum_{i=1,2} \rho(\mathbf{n}_0'(\mathbf{e}_i)) \frac{d\sigma(\mathbf{k}, \mathbf{e}_i; \mathbf{k}')}{d\Omega_{\mathbf{k}'}} \Big[\sum_i \frac{d\sigma(\mathbf{k}, \mathbf{e}_i; \mathbf{k}')}{d\Omega_{\mathbf{k}'}} \Big]^{-1}. \quad (3.8)$$

In Eq. (3.10), $\rho(\mathbf{e})$ is the polarization density matrix of a photon[63] with polarization vector **e** whose matrix elements are given by the formula

$$\rho_{ik} = e_i e_k^*, \quad (3.9)$$

where $\mathbf{e}_i$ are the coefficients in expansion of the polarization vector in the polarization basis vectors. For example, from Eq. (2.4), $\mathbf{e}_1 = i \sin \alpha_M e^{iM\varphi}$, $\mathbf{e}_2 = \cos \alpha_M e^{iM\varphi}$.

In the case of partially polarized radiation with a degree of polarization P, the scattering cross section is represented in the form

$$\Big(\frac{d\sigma}{d\Omega_{\mathbf{k}'}}\Big)_P = (1 - P) \frac{d\sigma}{d\Omega_{\mathbf{k}'}} + P \frac{d\sigma(\mathbf{k}, \mathbf{e}; \mathbf{k}')}{d\Omega_{\mathbf{k}'}}, \quad (3.10)$$

where **e** is the vector of the polarization partially represented in the radiation. The polarization density matrix of the scattered radiation turns out to be

$$\rho_P = \Big[(1 - P) \frac{d\sigma}{d\Omega_{\mathbf{k}'}} \rho + P \frac{d\sigma(\mathbf{k}, \mathbf{e}; \mathbf{k}')}{d\Omega_{\mathbf{k}'}} \rho(\mathbf{n}_0')\Big] \times \Big[(1 - P) \frac{d\sigma}{d\Omega_{\mathbf{k}'}} + P \frac{d\sigma(\mathbf{k}, \mathbf{e}; \mathbf{k}')}{d\Omega_{\mathbf{k}'}}\Big]^{-1}. \quad (3.11)$$

The formulas given above for polarization and cross sections refer to scattering of monochromatic γ rays. In view of the resonance nature of nuclear scattering, these expressions are rapid functions of the γ-ray energy E_γ. In order to take into account the finite width of the initial radiation line, expressions (3.8) and (3.11) must be integrated over energy with a weighting factor I(E) which describes the shape of the initial radiation line.

For example, the polarization density matrix ρ_P with inclusion of the finite width of the line is given by the expression

$$\bar{\rho}_P = \frac{\int I(E) (d\sigma/d\Omega_{\mathbf{k}'})_P \rho_P(E)\, dE}{\int I(E) (d\sigma/d\Omega_{\mathbf{k}'})_P\, dE}. \quad (3.12)$$

Here we have introduced into the quantities defined above an argument E, in order to emphasize their dependence on energy. Since, as a result of the interference of Rayleigh and nuclear scattering in the crystalline peaks, ρ_P is a function of E_γ, it follows from Eq. (3.12) that for these peaks, even in the case of completely polarized incident radiation, the scattered radiation turns out to be partially polarized. In the nuclear peaks, where ρ_P does not depend on E_γ, in the case of polarized incident radiation $\bar{\rho}$ corresponds to completely polarized scattered radiation.

The general structure of the cross section for scattering of unpolarized radiation in a magnetically ordered crystal and its energy dependence, as before, can be represented in the form of Eq. (3.3). However, in this case the nature of the dispersion curves determined

by the third term in Eq. (3.3) turns out to depend on the type of magnetic ordering in the crystal, the Zeeman transition through which the scattering mainly occurs, and the orientation of the magnetic fields in the Mössbauer nuclei. This follows directly from the corresponding dependences of the coherent amplitude (see Eq. (2.8)).

f) Completely resolved Zeeman splitting of the Mössbauer line. We will now consider the explicit form of the general expressions given above for the case of several types of magnetic ordering in crystals. For simplicity we will assume that the Zeeman splitting in the crystal is much greater than the line width of the scattered radiation and the Mössbauer line width in the crystal, i.e., the nuclear scattering occurs through completely determined Zeeman levels of the ground and excited states of the nucleus. The differential cross sections for scattering of unpolarized γ rays for electric dipole E1 and magnetic dipole M1 nuclear transitions are determined by the following expressions:

1) Ferromagnetic crystals. In this case the magnetic unit cell is identical to the crystalline unit cell and there are no magnetic diffraction peaks. Using Eq. (3.1), we obtain the following expressions for the nuclear and interference components of the cross section. The nuclear term is

$$\sigma_f^N = \frac{C^2(\mathbf{k},\mathbf{k}')\,\Gamma^2\,|\widetilde{F}_\tau^N|^2}{2k^2(1+M^2)^2\,|\Delta E|^2}[1-(-1)^M\cos^2\theta]\,[1-(-1)^M\cos^2\theta']. \quad (3.13)$$

The interference term σ^{RN} is given by the following expressions for the case of the transition multipolarities listed:

a) for an M1 transition,

$$\sigma_f^{RN} = \frac{r_e}{k}\frac{C(\mathbf{k},\mathbf{k}')\,\Gamma}{(1+M^2)\,|\Delta E|^2}\left\{\left[\frac{1}{4}\sin 2\theta\sin 2\theta'\cos\Phi+\sin^2\theta\sin^2\theta'\right.\right.$$
$$\left.+M^2(\cos^2\theta+\cos^2\theta'-\sin^2\theta\sin^2\theta'\sin^2\Phi)\right]\mathrm{Re}\,(\Delta E\widetilde{F}_\tau^{N*}F_\tau^R) \quad (3.14a)$$
$$\left.-M\left(\frac{1}{4}\sin 2\theta\sin 2\theta'\sin\Phi+\frac{1}{2}\sin^2\theta\sin^2\theta'\sin 2\Phi\right)\mathrm{Im}\,(\Delta E\widetilde{F}_\tau^{N*}F^R)\right\};$$

b) For an M1 transition,

$$\sigma_f^{RN} = \frac{r_e}{k}\frac{C(\mathbf{k},\mathbf{k}')\,\Gamma}{(1+M^2)\,|\Delta E|^2}[\sin\theta\sin\theta'\cos\Phi\,\mathrm{Re}\,(\Delta E\widetilde{F}_\tau^{N*}F^R)+$$
$$+2M^2\cos\theta\cos\theta'\,\mathrm{Re}\,(\Delta E\widetilde{F}_\tau^{N*}F^R)-M\sin\theta\sin\theta'\sin\Phi\,\mathrm{Im}\,(\Delta E\widetilde{F}_\tau^{N*}F_\tau^R)], \quad (3.14b)$$

where

$$C(\mathbf{k},\mathbf{k}')=\frac{3p\Gamma_{mm'}f(\mathbf{k})f(\mathbf{k}')}{8\Gamma(2j+1)}, \quad \widetilde{F}_\tau^N=\sum_q e^{i(\mathbf{k}-\mathbf{k}')\mathbf{r}_q},$$

where the summation is carried out within the unit cell only over the Mössbauer nuclei, $\Delta E = E_\gamma - E_{mm'} + (i\Gamma/2)$, $\Phi = \varphi - \varphi'$ is the difference in the azumithal angles of the vectors $\mathbf{k}$ and $\mathbf{k}'$ (the Z axis is directed along the magnetic field; see Fig. 2), and the remaining designations are the same as above.

Equations (3.14) show that the explicit form of the interference term depends on the crystal structure and is different for the different lines of the Mössbauer spectrum. The interference term is different also for electric and magnetic types of dipole nuclear transition. The latter difference is due to the fact that Rayleigh scattering is electric dipole, and therefore the result of its interference with nuclear scattering turns out to be different for E1 and M1 transitions. The dependence noted of the form of the interference term on the transition multipolarity can in principle be used to determine the type of nuclear transition.

2) Antiferromagnetic crystals. The magnetic field in the nuclei takes on two values, H and $-H$. At a magnetic maximum in expression (3.1) only the nuclear term is different from zero,

$$\sigma_{of}^N=\frac{M^2C^2(\mathbf{k},\mathbf{k}')\,\Gamma^2}{2k^2\,|\Delta E|^2}\,|\widetilde{F}_H^N|\,(\cos^2\theta+\cos^2\theta'+\sin^2\theta\sin^2\theta'\sin^2\Phi), \quad (3.15)$$

where $\widetilde{F}_H^N = \sum_q e^{(i\mathbf{k}-\mathbf{k}')\mathbf{r}_q}$, and the summation is carried out within the unit cell over nuclei located in a field H.

The nuclear term for the crystalline peaks is

$$\sigma_{of}^N=\frac{C^2(\mathbf{k},\mathbf{k}')\,\Gamma^2}{2k^2(1+M^2)^2\,|\Delta E|^2}\{[1-(-1)^M\cos^2\theta]\,[1-(-1)^M\cos^2\theta']\,(|\widetilde{F}_H^N|^2+|\widetilde{F}_{-H}^N|^2)$$
$$+2\sin^2\theta\sin^2\theta'\,\mathrm{Re}\,(\widetilde{F}_H^N\widetilde{F}_{-H}^{N*}e^{i2M\Phi})\}. \quad (3.16)$$

The interference term for E1 and M1 transitions is given respectively by expressions (3.14a) and (3.14b) if the expression under the Re sign in them is replaced by $\Delta E F^R(\widetilde{F}_H^{N*}+\widetilde{F}_{-H}^{N*})$, and the expression under the Im sign is replaced by $\Delta E F^R(\widetilde{F}_H^{N*}-\widetilde{F}_{-H}^{N*})$.

We note that for $M = 0$, as shown by Eq. (3.15) there are no magnetic peaks. This result turns out to be independent of the transition multipolarity and is due to the fact that in this case the Mössbauer scattering amplitude does not change on replacement of H by $-H$.

As follows from the general discussion, the polarization characteristics of the radiation scattered in the diffraction peaks depend on interference of nuclear and Rayleigh scattering and, in particular, depend on the ratio of the corresponding structure factors and the shape of the Mössbauer radiation line. Therefore we will limit ourselves to presenting the explicit form of the polarization density matrix only for the nuclear diffraction peaks, for which the Rayleigh structure factor goes to zero, and the energy averaging (3.12) does not change the form of the polarization density matrix.

We have given below the polarization characteristics of radiation in the magnetic peaks in the case of an antiferromagnetic crystal. The corresponding polarization density matrix, as follows from the remark made above, is the same over the entire width of the Mössbauer line. In the case of polarized primary radiation with a polarization vector $\mathbf{e}$ we find for the polarization vector of the scattered radiation from Eq. (2.8), (3.5), and (3.6)

$$\mathbf{n}_0'=\frac{\mathbf{N}}{|N|}, \quad \mathbf{N}=\mathbf{n}_t(\mathbf{k}')\,(\mathbf{e}\mathbf{n}_t^*(\mathbf{k}))-\mathbf{n}_t^*(\mathbf{k}')\,(\mathbf{e}\mathbf{n}_t(\mathbf{k})). \quad (3.17)$$

For unpolarized incident radiation the polarization matrix is determined by Eq. (3.8) and, for M1 transitions in the basis vectors given by Eq. (2.5) (for the k' direction), has the following Stokes parameters:

$$\left.\begin{aligned}\xi_1&=\rho_{12}+\rho_{21}=\frac{\sin^2\theta\sin^2\theta'\sin 2\Phi}{\cos^2\theta+\cos^2\theta'+\sin^2\theta\sin^2\theta'\sin^2\Phi},\\ \xi_2&=i(\rho_{12}-\rho_{21})=0,\\ \xi_3&=\rho_{11}-\rho_{22}=\frac{\cos^2\theta'-\cos^2\theta-\sin^2\theta\,(1+\cos^2\theta')\sin^2\Phi}{\cos^2\theta+\cos^2\theta'+\sin^2\theta\sin^2\theta'\sin^2\Phi}.\end{aligned}\right\} \quad (3.18)$$

The degree of polarization of the scattered radiation is $P = \sum_{i=1}^{3}\xi_i^2$.

To obtain the corresponding expressions in the case of an E1 transition it is sufficient to change the signs of ξ_1 and ξ_2. The density matrix (3.18) is real. Physically this means that in the scattered radiation linear polarization is partially represented. The corresponding polarization vector forms with the basis vector χ_1' an angle ϵ determined from the relation $\epsilon = (1/2)\,\mathrm{arc\,tg}\,(\xi_1/\xi_3) + (\pi/4)(1-\mathrm{sign}\,\xi_1)$. For $\xi_1 = 0$ the density matrix is diagonal in the basis vectors used and the scattered radia-

tion is partially polarized along one of them (for $\xi_3 > 0$, along χ_1', and for $\xi_3 < 0$, along χ_2'); for $\xi_1 = \xi_3 = 0$ the radiation is unpolarized. In particular, the radiation is polarized along one of the basis vectors χ_1', χ_2' if the magnetic field lies in the scattering plane or perpendicular to it. In the first case the degree of polarization is $P = |\cos^2\theta - \cos^2\theta_1'| \times (\cos^2\theta + \cos^2\theta)^{-1}$, and in the second case the radiation is completely polarized.

It should be noted that in the case considered the polarization density matrix of radiation scattered in the magnetic peaks in an antiferromagnetic crystal does not depend on the crystalline structure and is determined only by the magnetic structure of the crystal. Therefore on the basis of the polarization density matrix (3.20) measured at a magnetic peak it is possible to determine uniquely the orientation of the antiferromagnetic axis in the crystal. The polarization of the radiation in the crystalline peaks depends both on the magnetic structure and on the crystalline structure of the antiferromagnetic crystal. Therefore polarization measurements can be used to obtain information on the crystalline structure.[71] Inclusion of absorption[72,73], and also the results of a similar discussion of diffraction in more complex magnetic structures and polycrystalline materials and specific compounds, are given in refs. 49, 50, and 74.

g) **Crystals containing Mössbauer nuclei in sites with a nonuniform electric field.** In the case of diffraction in crystals containing Mössbauer nuclei in sites with a nonuniform electric field, as a result of the dependence of the coherent nuclear amplitude on the electric field gradient, the intensity of the diffraction peaks and the polarization of the radiation in them contain information on the electric field gradient and can be used in structure research.[42] This information can be particularly useful in study of phase transitions accompanied by small distortions of the crystalline unit cell, which are difficult to detect by traditional diffraction methods, for example, in the case of segnetoelectric transitions. We will not dwell in detail on this case[42] but will limit ourselves to discussion of diffraction in crystals for which there are quadrupole diffraction peaks, which are absent in scattering of radiation of other types.[48] Just as the dependence of the scattering amplitude on magnetic field leads to the existence of magnetic diffraction peaks, a consequence of the dependence of the Mössbauer scattering amplitude on the orientation of the principal axes of the electric field gradient tensor turns out to be the existence in Mössbauer scattering of quadrupole diffraction peaks, which are forbidden by the crystalline space group. Quadrupole diffraction peaks exist for crystals in which Mössbauer nuclei located at crystallographically equivalent positions are acted on by electric field gradients differing in the spatial orientation of their principal axes. The dependence of the Mössbauer amplitude on the orientation of the electric field gradient tensor axes makes Mössbauer nuclei located at equivalent crystallographic positions nonequivalent in scattering (Fig. 5), which also leads to appearance of diffraction peaks forbidden by the crystalline space group. For the structure factor (3.3) this means that there exist reciprocal-lattice vectors τ for which $F_\tau^N \neq 0$, while $F_\tau^R \equiv 0$ for reasons of symmetry. As an example of such a structure, we can mention sodium nitroprusside, in which quadrupole peaks were observed experimentally for the first time.[52]

We note that nonequivalence similar to that discussed above in the scattering of atoms located at equivalent crystallographic positions may be due to anisotropy of thermal lattice vibrations. In this case there exist dynamical diffraction peaks forbidden by the crystalline space group.[52,75]

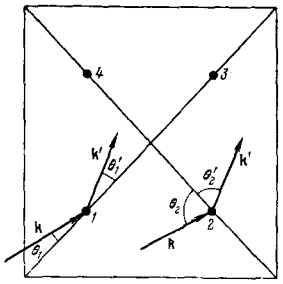

FIG. 5. Schematic illustration of the nonequivalence in scattering by nuclei occupying crystallographically equivalent sites 1, 2 (3, 4). The principal axis of the electric field gradient tensor coinciding with the diagonal of the unit cell at sites 1, 2 (3, 4) is oriented differently, as a consequence of which the nuclear resonance scattering amplitudes for these sites are different.

4. DYNAMICAL THEORY OF MÖSSBAUER DIFFRACTION

a) **The system of dynamical equations.** In the previous section we discussed Mössbauer diffraction in the kinematic approximation. This approximation is applicable for a quantitative description to thin crystals with a thickness $L < V/\sigma_{coh}$, where σ_{coh} is determined by Eq. (2.11) and V is the volume of the crystal unit cell. This means, for example, that in the case of the 14.4-keV transition in Fe^{57} for 100% content of the Mössbauer isotope in the crystal at the exact resonance, $L \sim 10^{-4}$ cm. On departure from the exact resonance and reduction of the concentration of the Mössbauer isotope, L increases as

$$p^{-2}\left|\frac{E-E_0}{\Gamma}+\frac{i}{2}\right|^2;$$

for the natural content of the Mössbauer isotope (p = 0.025) at the exact resonance, L turns out to be of the order 10^{-2} cm.

In the general case, for quantitative description of the diffraction pattern it is necessary to take into account multiple scattering and the attenuation of the γ-ray beam as it is propagated through the crystal. These factors are taken into account by the dynamical theory of diffraction. The dynamical theory not only describes quantitatively diffraction by perfect crystals, but also leads to a number of qualitatively new results which are absent in the kinematic approximation. Among these are the suppression of inelastic nuclear-reaction channels in propagation of γ rays in a crystal in the case where the Bragg condition is satisfied (the Kagan-Afanas'ev effect), oscillations with thickness of the intensity of the γ rays which have passed through the crystal (Pendellosung), and so forth. These effects have direct analogies in x-ray diffraction, but, as a result of the specific nature of the interaction of Mössbauer γ rays with nuclei, their appearance in Mössbauer diffraction has important features. For example, the suppression of inelastic nuclear-reaction channels turns out to be independent of the crystal temperature, while the corresponding x-ray analog, the anomalous transmission of x rays (the Bormann effect) has a strong temperature dependence.

The equation of the dynamical theory of Mössbauer diffraction can be obtained both from classical[22,27] and quantum-mechanical considerations.[25,28] We will give below a classical derivation of these equations, referring those interested in the quantum derivation to the references cited.

The Maxwell equations describing the propagation of γ rays in a crystal we will write in the form

$$\operatorname{rot} \mathbf{H} = \frac{1}{c}\frac{\partial \mathbf{D}}{\partial t}, \quad \operatorname{div} \mathbf{D} = 0, \quad \operatorname{rot} \mathbf{E} = -\frac{1}{c}\frac{\partial \mathbf{H}}{\partial t}, \quad \operatorname{div} \mathbf{H} = 0, \quad (4.1)$$

assuming a magnetic permeability $\mu = 1$. Then, using the relation between induction and electric field strength written in the form $\partial \mathbf{D}/\partial t = \partial \mathbf{E}/\partial t + 4\pi \mathbf{j}$ where $\mathbf{j}$ is the current density induced by the fields $\mathbf{E}$ and $\mathbf{H}$, for the Fourier components of $\mathbf{E}$ and $\mathbf{j}$ we arrive at the equation

$$\left(k^2 - \frac{\omega^2}{c^2}\right)\mathbf{E}(\mathbf{k}, \omega) - \mathbf{k}(\mathbf{k}\mathbf{E}(\mathbf{k}\omega)) = i\frac{4\pi}{c^2}\omega \mathbf{j}(\mathbf{k}\omega). \quad (4.2)$$

As a result of the periodicity of the medium, the current harmonic $\mathbf{j}(\mathbf{k}, \omega)$ is induced not only by the field harmonic $\mathbf{E}(\mathbf{k}\omega)$ but also by field harmonics with wave vectors $\mathbf{k}_\tau$ differing from $\mathbf{k}$ by any reciprocal-lattice vector τ. Therefore, expressing $\mathbf{j}(\mathbf{k}\omega)$ in terms of $\mathbf{E}(\mathbf{k}_\tau\omega)$, we obtain from Eq. (4.2) an infinite system of linear equations for the amplitudes $\mathbf{E}(\mathbf{k}\omega)$ and $\mathbf{E}(\mathbf{k}_\tau\omega)$, where $\mathbf{k}_\tau = \mathbf{k} + \tau$. As is well known, the amplitude $\mathbf{E}(\mathbf{k}_\tau\omega)$ turns out to be of the same order as $\mathbf{E}(\mathbf{k}\omega)$ if $|\mathbf{k}_\tau| \cong\approx |\mathbf{k}|$; in the opposite case it turns out to be small. We will further assume that the condition $|\mathbf{k}_\tau| \cong\approx |\mathbf{k}|$ is satisfied for the single vector $\mathbf{k}_\tau$ and therefore the equations (4.2) can be reduced approximately to a system of equations of only two such amplitudes. This approximation is called the two-wave approximation and is widely used in the dynamical theory of x-ray diffraction.[76] Thus, limiting ourselves to two Fourier components $\mathbf{E}_{\mathbf{k}_1}$ and $\mathbf{E}_{\mathbf{k}_2}$, where $\mathbf{k}_2 = \mathbf{k}_1 + \tau$, and using the smallness of the nontransversality of the electromagnetic field in the crystal, we arrive at the following system of two vector equations involving $\mathbf{E}_{\mathbf{k}_1}$ and $\mathbf{E}_{\mathbf{k}_2}$:

$$\begin{aligned}\left(\frac{k_1^2}{\kappa^2} - 1\right)\mathbf{E}_{\mathbf{k}_1} &= \hat{F}_{11}\mathbf{E}_{\mathbf{k}_1} + \hat{F}_{12}\mathbf{E}_{\mathbf{k}_2},\\ \left(\frac{k_2^2}{\kappa^2} - 1\right)\mathbf{E}_{\mathbf{k}_2} &= \hat{F}_{21}\mathbf{E}_{\mathbf{k}_1} + \hat{F}_{22}\mathbf{E}_{\mathbf{k}_2}.\end{aligned} \quad (4.3)$$

In the equations (4.3) $\omega/c = \kappa$ is the γ-ray wave vector in vacuum, and $\hat{F}$ is a vector operator whose elements $F_{sp}^{\mu'\mu}$ describe the coherent scattering by the unit cell of a γ ray with wave vector $\mathbf{k}_p$ and polarization μ into a γ ray with wave vector $\mathbf{k}_s$ and polarization μ'. The explicit form of the operator F we will discuss below. The four solutions of the homogeneous system of two vector equations (4.3) define four eigenconfigurations of the field in the crystal near the Bragg condition, i.e., $\mathbf{n}$, $\mathbf{n}'$ are the eigenpolarization vectors of the waves $\mathbf{E}_1 \equiv \mathbf{E}_{\mathbf{k}_1}$, $\mathbf{E}_2 \equiv \mathbf{E}_{\mathbf{k}_2}$, and their wave vectors $\mathbf{k}_1$, $\mathbf{k}_2 = \mathbf{k}_1 + \tau$, and also the ratio of the amplitudes E_1 and E_2. The general solution of Maxwell's equations in the crystal $\vec{\mathcal{E}}(\mathbf{r}, t)$ is represented by a superposition of the eigensolutions:

$$\vec{\mathcal{E}}(\mathbf{r}, t) = \sum_p C_p [\mathbf{n}_p E_1^p \exp(i\mathbf{k}_1^p\mathbf{r}) + \mathbf{n}_p' E_2^p \exp(i\mathbf{k}_2^p\mathbf{r})] \exp(-i\omega t). \quad (4.4)$$

where C_p are the expansion coefficients of the field in the crystal in the eigensolutions, and the index p takes on values from 1 to 4 and enumerates the eigensolutions. The coefficients C_p in Eq. (4.4) and the values of the wave vectors $\mathbf{k}_i^p$ of the waves excited in the crystal are found by means of the boundary conditions.

The difference of the system (4.3) from the corresponding equations of the dynamical theory of x-ray diffraction lies in the form of the operator $\hat{F}$. Specifically, for Mössbauer diffraction it is necessary to add to the expression for $\hat{F}$ in the x-ray case[76], which describes the scattering of photons by electrons, a term associated with nuclear scattering. Thus, in Eq. (4.3) we have $\hat{F} = \hat{F}^R + \hat{F}^N$, where $\hat{F}^R$ and $\hat{F}^N$ are its parts associated with Rayleigh and nuclear resonance scattering, respectively. The nuclear component $\hat{F}^N$ is determined by the coherent amplitude of nuclear scattering[22, 29, 46] and is related to the coherent-scattering tensor of the unit cell, introduced and used above (3.5), by the relation

$$F_{sp}^{\mu'\mu} = \frac{4\pi}{Vk^2} T_{\mu'\mu}^{sp}. \quad (4.5)$$

where p and s denote the directions of propagation of the incident and scattered γ rays, and μ and μ' are the polarization indices corresponding to them.

We will begin our analysis of the system of dynamical equations with the simplest assumption as to the form of the tensor $\hat{T}$, which is realized in the case of an unsplit Mössbauer line.

b) Unsplit Mössbauer line. In this case in the polarization basis vectors π and σ the operator $F_{sp}^{\mu'\mu}$ is diagonal in the spin indices μ, μ' and by means of Eqs. (3.3) and (4.5) can be represented in the form

$$\hat{F}^N = \frac{4\pi}{Vk^2}\begin{pmatrix} F_0^N & P^N F_\tau^N \\ P^N F_{-\tau}^N & F_0^N \end{pmatrix}, \quad (4.6)$$

where F_τ^N is the nuclear structure factor defined by Eq. (3.4).

The explicit form of the polarization factor P^N for dipole nuclear transitions follows from Eq. (2.9) and is given in the explanations of Eq. (3.4).

In the case considered, the solutions of the system (4.3) are completely analogous to the corresponding solutions for x rays. Specifically, the eigenpolarizations are the polarizations π and σ and the system of vector equations breaks up into two uncoupled systems of scalar equations which determine $\mathbf{k}_1$, $\mathbf{k}_2$, and E_1/E_2 for the σ and π polarizations:

$$\begin{aligned}\left(\frac{k_1^2}{\kappa^2} - 1\right)E_1 &= F_{11}E_1 + F_{12}^{\mu}E_2,\\ \left(\frac{k_2^2}{\kappa^2} - 1\right)E_2 &= F_{21}^{\mu}E_1 + F_{22}E_2,\end{aligned} \quad (4.7)$$

where the index μ takes on two values corresponding to σ and π polarizations and F_{ik}^{μ} is the sum of the Rayleigh[76] and nuclear (4.6) terms.

The condition of solubility of the system (4.7) (equality to zero of its determinant) for each eigensolution determines the region of values of $\mathbf{k}_1$ and $\mathbf{k}_2$ compatible with the Bragg condition (3.2) and satisfying Maxwell's equations. These regions in k space, according to the number of eigensolutions, form four so-called dispersion surfaces.[76, 114] Each point of a dispersion surface corresponds to a value of E_2/E_1. In the case discussed two eigensolutions of the system (4.7) correspond to each polarization σ and π, i.e., two dispersion surfaces. Thus, in contrast to the kinematic approximation, in the dynamical theory the secondary diffracted wave exists not for a single value of the angle between $\mathbf{k}_1$ and $\mathbf{k}_2$, but in some small interval of angles $\Delta\theta$ near the Bragg condition. The size of the interval $\Delta\theta$ determines the parameters characterizing the interaction strength of the γ ray with the crystal,[76] i.e., F_{ik}^{μ}.

In what follows we will not dwell on a detailed analysis of the eigensolutions of the system (4.7) and the dispersion surfaces corresponding to them, but, following ref. 22, we will give a solution which immediately satisfies the boundary conditions. For this purpose we will assume that the crystal has the form of a plane parallel plate. The wave vectors $\mathbf{k}_1$ and $\mathbf{k}_2$ we will write in the form

$$\mathbf{k}_1 = \varkappa + \varkappa\zeta\mathbf{s}, \quad \mathbf{k}_2 = \mathbf{k}_1 + \tau, \tag{4.8}$$

where $\mathbf{s}$ is the inwardly directed normal to the crystal surface, and ζ is a small quantity. We will relate k_1 and k_2 to the angle of incidence of the γ ray on the crystal $\theta_1 = \widehat{\varkappa\mathbf{s}} \approx (\widehat{\mathbf{k}_1\mathbf{s}})$. For this variation we will represent k_1 and k_2, in comparison with the vacuum quantity κ, in the form

$$k_1 = \varkappa(1+\varepsilon_1), \quad k_2 = \varkappa(1+\varepsilon_2), \quad \zeta = \varepsilon_1/\cos\theta_1, \quad |\varepsilon_1|, \ |\varepsilon_2| \ll 1. \tag{4.9}$$

Substituting (4.8) and (4.9) into (4.7), from the condition of solubility of the system we find

$$\varepsilon_1 = \frac{1}{4}(F_{11} + bF_{22} - b\delta) \pm \frac{1}{4}\sqrt{(F_{11} + bF_{22} - b\delta)^2 + 4b[F_{11}\delta - (F_{11}F_{22} - F_{12}^{\mu}F_{21}^{\mu})]}, \tag{4.10}$$

$$\varepsilon_2 = \frac{\delta}{2} + \frac{\varepsilon_1}{b},$$

where $b = \cos\theta_1/\cos\theta_2$, $\theta_2 = (\widehat{\mathbf{k}_2\mathbf{s}})$, $\delta = \tau(\tau + 2\varkappa)/\varkappa^2$.

The parameter δ is a measure of the deviation from the Bragg condition.

The values of ϵ_1 which have been found correspond to the following ratio of the amplitudes of the waves in the eigensolutions:

$$R = B^2 = \frac{|E_2|^2}{|E_1|^2} = \left|\frac{2\varepsilon_1 - F_{11}}{F_{12}^{\mu}}\right|^2. \tag{4.11}$$

From Eqs. (4.10) and (4.11) it follows that $|E_2|^2/|E_1|^2 \sim 1$ in the region of angles $\Delta\theta \sim |F_{12}^{\mu}|$ (for more details see ref. 76).

The solution given for the system (4.7), like the solution of the corresponding system for x rays, also in the case of an unsplit Mössbauer line, permits description of all features of Mössbauer coherent scattering due to the existence of resonance nuclear scattering.

In what follows we will discuss individually diffraction in a crystal in the Bragg case (primary and diffracted rays are on the same side of the entrance surface of Fig. 6a) and in the Laue case (primary and diffracted rays are on opposite sides of the crystal surface, Fig. 6b). To simplify the formulas, we assume that the crystal surface is parallel (in the Bragg case) or perpendicular (in the Laue case) to the reflecting plane of the crystal or, as one says, symmetric cases of diffraction occur. In the Laue case the boundary conditions have the form

$$\sum_p C_p \mathbf{u}_p' E_2^p = 0, \quad \vec{\mathcal{E}}_0 = \sum_p C_p \mathbf{u}_p E_1^p, \tag{4.12}$$

where $\mathcal{E}_0$ is the amplitude of the wave incident on the crystal.

In the Bragg case the boundary conditions have the form

$$\sum_p C_p \mathbf{u}_p E_1^p = \vec{\mathcal{E}}_0, \quad \sum_p C_p \mathbf{u}_p' E_2^p \exp(i\mathbf{k}_2^p \mathbf{s} L) = 0, \tag{4.13}$$

where L is the crystal thickness.

c) **Suppression of inelastic nuclear-reaction channels.** Without writing out in explicit form the coefficients C_p in the expansion (4.4), which are found from the boundary conditions (4.12), we will analyze how the individual terms of the expansion (4.4) are damped in space for the symmetric Laue case (b = 1).

Far from the Bragg condition, $|\delta| \gg 1$, the wave amplitude E_2 is negligible, and therefore the wave E_1 is propagated in the crystal.

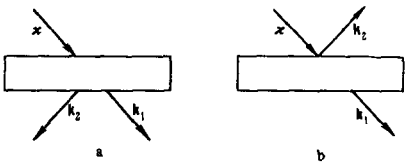

FIG. 6. Diagram of diffraction experiment in the Laue case (a) and Bragg case (b).

The wave vector k_1 corresponding to it is determined by Eq. (4.10) with the plus sign in front of the radical, i.e., $k_1 = \kappa[1 + (1/2)F_{11}]$. The wave corresponding to the minus sign in Eq. (4.10) is not excited in the crystal.[22,76] The damping of the wave is determined by the imaginary part of the wave vector k_1. Far from the Bragg condition it turns out to be equal to $(1/2)\kappa \mathrm{Im}\, F_{11}$. Neglecting in this expression the damping due to the interaction of the γ rays with the electrons, we obtain for the intensity of the wave as a function of its depth of penetration x the usual expression:

$$I \sim \exp(-\mu x), \quad \mu = \varkappa \mathrm{Im}\, F_{11} = \frac{\sigma_T}{V}, \tag{4.14}$$

where σ_T is the total resonance cross section for absorption of γ rays in the crystal, determined by Eq. (2.10).

Near the Bragg condition ($|\delta| \lesssim |F_{ik}^{\mu}|$) in the expansion (4.4) in the general case all four eigensolutions are represented. However, the damping of the different eigenwaves in the crystal can differ substantially. The damping of two of the eigenwaves can significantly decrease in comparison with the damping off the Bragg condition and, for certain values for one of them, even go to zero.

In order to convince ourselves of this, let us consider the propagation of a wave in the crystal for a value of the parameter Δ small in comparison with $|F_{ik}^{\mu}|$:

$$\Delta = F_{11}F_{22} - F_{21}F_{12}. \tag{4.15}$$

In this case the upper of Eqs. (4.10) can be written approximately in the form

$$\varepsilon_1^- = -\frac{1}{2}\frac{F_{11}\delta - \Delta}{F_{11} + F_{22}}, \quad \varepsilon_1^+ = \frac{1}{2}\left(F_{11} + F_{22} - \delta + \frac{F_{11}\delta - \Delta}{F_{11} + F_{22}}\right), \tag{4.16}$$

where the upper index in ϵ_1 corresponds to the sign in front of the radical in Eq. (4.10). As follows from Eq. (4.16), the eigensolutions and the corresponding terms in the expansion (4.4) corresponding to ϵ_1^+ have a damping coefficient of the same order as Eq. (4.14). The second pair of eigensolutions, corresponding to ϵ_1^-, are damped substantially more weakly, with an absorption coefficient equal to

$$\mu^- = 2\mathrm{Im}\, \varkappa\varepsilon^-. \tag{4.17}$$

This means that under the conditions discussed γ rays can penetrate through the thickness of the crystals substantially more than off the Bragg condition. This phenomenon is well known in x-ray diffraction and is called the Bormann effect. In Mössbauer diffraction it is known as the suppression of inelastic nuclear-reaction channels, or the Kagan-Afanas'ev effect. The physical nature of the two effects mentioned is similar. Under diffraction conditions the wave incident on the crystal is essentially transformed so that the electromagnetic field in the crystal is the coherent superposition of two plane waves. Here

the phase relations of these waves are such that for the two eigensolutions the minima of the electric or magnetic field strength (depending on the multipolarity of scattering) occurs at the crystal lattice sites. This leads to a decrease in the cross sections for inelastic processes, the photoeffect in the atoms, and resonance absorption of γ rays in the nuclei, and produces the observed reduction in absorption coefficient.

However, as a result of the substantial difference in the characteristic times of Rayleigh and nuclear resonance scattering, there is a qualitative difference in the appearance of these effects. We recall that the time of resonance scattering in a nucleus $\tau_N \sim 10^{-7}$ sec is substantially greater than the inverse frequencies of lattice vibrations $\tau_p \sim 10^{-12}$ sec, while the time of Rayleigh scattering by an electron is substantially less than τ_p. While it is possible to achieve a complete suppression of inelastic reaction channels in the Kagan-Afanas'ev effect, in the case of the Bormann effect complete suppression of inelastic processes is impossible in principle.

The condition of complete suppression of inelastic processes is the simultaneous vanishing of μ^- for π and σ polarizations. As follows from Eq. (4.10), this is possible only for $\delta = 0$ and $\Delta = 0$.

In the case of scattering by electrons, vanishing of Δ is impossible, since as a result of the ratio cited of the characteristic times of lattice vibrations and the scattering time the amplitudes F^R_{ik} contain Debye-Waller factors, which for F^R_{ii} (scattering at zero angle) are identically equal to unity, and for F^R_{ip}, $i \neq p$, are always less than unity. In the case of Mössbauer scattering as a result of the slowness of the process the quantities F^N_{ip} contain not Debye-Waller factors, but Lamb-Mössbauer factors in the form $\exp(-k_i^2\langle x_{k_i}^2\rangle)\exp(-k_p^2\langle x_{k_p}^2\rangle)$, whose product turns out to be identical for the two terms in Eq. (4.15) and does not prevent a strict vanishing of Δ. For example, for the case discussed of an unsplit Mössbauer line, complete suppression of inelastic channels turns out to be possible (neglecting Rayleigh scattering) for the σ polarization if the Mössbauer transition is electric dipole and for the π polarization if the transition is magnetic dipole.[22]

The same ratio of the scattering times and inverse vibration frequencies of the lattice also explains the absence of a temperature dependence in the Kagan-Afanas'ev effect and the strong temperature dependence (decrease in anomalous transmission with increasing temperature) for the Bormann effect. In the Rayleigh case Δ actually increases with increasing temperature, since the first term in Eq. (4.15) does not change, and the second decreases with increasing temperature. In the Mössbauer case a change in temperature does not lead to a departure of Δ from zero, since the thermal factors in Eq. (4.15) turn out to be identical for the two terms.

It should be noted that since the suppression of inelastic nuclear-reaction channels appears in a region of angles $\Delta\theta \lesssim |F_{12}|$ near the Bragg condition, which amounts to several seconds of arc, it is desirable for experimental observation of this effect to use a γ-ray beam with collimation of the same order, and also crystals of a high degree of perfection.[22, 35, 37]

d) Bragg reflection from crystals. We will now analyze the solution of the problem of diffraction reflection in the

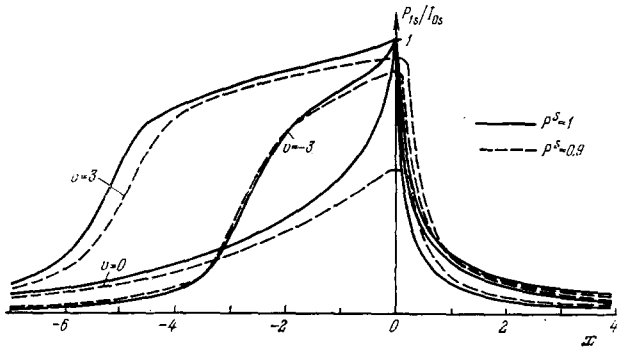

FIG. 7. Theoretical angular dependence of Bragg reflection by a perfect crystal for three values of the parameter $v = [2(E_\gamma - E_0)]/\Gamma$ (ref. 26). The variation in angle is characterized by the parameter $x = (1/F_{11} - \mathrm{Re}\, F_{12}\rho^S)]$.

symmetric Bragg case ($b = -1$). We will not write out the expansion (4.4) for crystals of arbitrary thickness,[26] but for the sake of simplicity we will limit ourselves to thick crystals for which $|L\kappa \mathrm{Im}(\epsilon^+ - \epsilon^-)| \gg 1$. As for x rays, in this case only two eigenwaves will be represented in the expansion (4.4), the values of whose wave vectors are determined[26, 27] by the quantities ϵ^+. Therefore, if the wave incident on the crystal has π (or σ) polarization, its coefficient of reflection from the crystal R is determined simply by the ratio (4.11) for the eigensolution with π (or σ) polarization corresponding to ϵ^+. Hence it follows that if $\Delta = 0$ for the eigenpolarization (see Eq. (4.15)), then for some value of the parameter δ for this polarization $|E_2|^2/|E_1|^2 = 1$, i.e., for the corresponding angle of incidence, total reflection occurs. This fact is the consequence of the complete suppression of the inelastic channels. In the x-ray case when inelastic processes are taken into account the ratio (4.11) does not go to unity, in view of the fact that complete suppression of inelastic processes does not occur and therefore a loss in the intensity of radiation on reflection is unavoidable. However, in contrast to the x-ray case, in which the absorption is small and the reflection coefficient is practically constant in the region of diffraction reflection and falls off sharply to zero outside this region, in the Mössbauer case the absorption is important and the reflection curve has the form shown in Fig. 7. Since the sum of the nuclear and Rayleigh scattering amplitudes and also the value of the absorption (the imaginary part of the coherent amplitude) depend substantially on the γ ray energy, then, as can be seen from Fig. 7, the shape of the reflection curve also depends on the value of the energy detuning from the exact resonance condition.

Since the angular size of the region of diffraction reflection is small and amounts to altogether about ten seconds of arc, and experiments are usually performed with γ-ray beams with a divergence significantly greater than this value, experiments usually observe the integrated reflected intensity:

$$R_T = \int \frac{|E_2|^2}{|E_1|^2}\, d\theta = \frac{1}{2\sin 2\theta_B} \int_{-\infty}^{+\infty} \frac{|E_2|^2}{|E_1|^2}\, d\delta. \qquad (4.18)$$

In the transition to the second part of the equality (4.18), the integration over angle is replaced in the usual manner by integration over the parameter δ with use of the relation $d\theta = -d\delta/2\sin 2\theta_B$, where $2\theta_B$ is the scattering angle when the Bragg condition (3.2) is satisfied.

Integration over δ in Eq. (4.18) with allowance for the smallness of Δ (see Eq. (4.15)) leads to a result[26] simi-

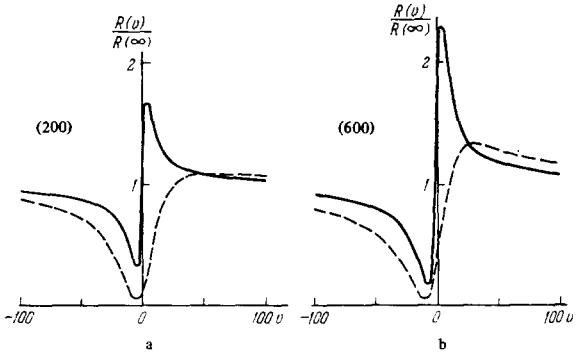

FIG. 8. Integral reflection coefficient for a perfect (solid curve) and imperfect (dashed curve) tin crystal enriched to 100%, calculated for the (200) (a) and (600) (b) reflections at a temperature of 77°K (ref. 26).

lar to the corresponding expression in x-ray diffraction theory[76]:

$$R_{T\mu}=\frac{8|F_{12}^{\mu}|}{3\sin 2\theta_B}\mathscr{F}^{\mu}, \qquad (4.19)$$

where the value of $\mathscr{F}^{\mu}$ is close to unity.

Let us consider the characteristic features of Mössbauer diffraction, which are due to the strong dependence of the amplitude F_{ik}^{N} on γ-ray energy. In the case of pure nuclear scattering, for example, it follows from expression (4.19) that for large detunings $v = (E_\gamma - E_0)/\Gamma$ the reflection coefficient is $R \sim 1/|v|$. This means that the dependence of the integrated reflection on v for a thick crystal turns out to be non-Lorentzian, and the energy width of the corresponding curve increases significantly in comparison with the case of a thin crystal, in which for $|v| \gg 1$ we have $R \sim 1/|v|^2$. The quantity F^{μ} in Eq. (4.19) also contains a smooth dependence on γ-ray energy and changes somewhat with change of the parameter v. The explicit form of this dependence has been given in ref. 26.

The appearance of interference between nuclear and Rayleigh scattering is characteristic for the reflection curve (see Fig. 7) and the integrated reflection coefficient. However, the interference of nuclear and Rayleigh scattering appears most clearly as a function of the detuning in the integrated reflected intensity (Fig. 8).

The formulas and illustrations presented above refer to diffraction in an ideal crystal. If a crystal possesses a significant mosaic structure, the energy dependence of the scattering changes.[26] For example, for a small secondary extinction the reflection coefficient from a thick mosaic crystal is given by the expression[20, 26]

$$R^{\mu}=\frac{\pi\varkappa|F_{12}^{\mu}|^2}{4\mu\delta\sin 2\theta_B}, \qquad (4.20)$$

where the absorption coefficient μ is defined by Eq. (4.14) and δ is the characteristic misalignment angle of the blocks in the crystal. Without going into a detailed analysis of the case of mosaic crystals, which can be described in terms of the kinematic approximation,[77] we will point out that the nature of the change of the interference pattern in comparison with the case of ideal crystals is illustrated by Fig. 8.

e) Eigensolutions of the dynamical system in the case of hyperfine splitting of the Mössbauer line. With the existence of hyperfine splitting of the Mössbauer line in a crystal (below for definiteness we will speak of magnetically ordered crystals), in the general case the system of dynamical equations (4.3) does not reduce to a system of two scalar equations for the amplitudes with known eigenpolarizations. Different eigenpolarizations[78] $\mathbf{n}_p$ and $\mathbf{n}_p'$ now correspond to each of the four solutions of the system (4.3). The eigenpolarizations (the vectors $\mathbf{n}_p$ and $\mathbf{n}_p'$) depend on the magnetic structure and do not remain constant within the diffraction region, but change with the degree of departure from the Bragg condition. Off the Bragg condition they go over to the eigenpolarizations for direct transmission.[58] In addition to the dependence of the eigenpolarizations on the angle of incidence of the γ ray on the crystal, in this case there is also a sharply expressed dependence of the eigenpolarizations on the γ-ray energy. In the limit of large deviations of the γ-ray energy from the resonance energy, when nuclear scattering can be neglected, the eigenpolarizations go over to the x-ray π and σ polarizations, and the specific properties of Mössbauer diffraction in magnetically ordered crystals disappear.

Thus, the nature of the diffraction pattern for magnetically ordered crystals is more complicated than the case selected above of crystals without magnetic ordering. Qualitatively new effects appear which are absent in diffraction for an unsplit Mössbauer line. For example, complete suppression of inelastic nuclear processes[79-91] turns out to be possible. The complication is mainly due to the polarization properties of the eigensolutions of the system (4.3).

In addition to the dependence noted above of the scattered radiation polarization on the magnetic structure of the crystal, a difference in the polarization properties of the eigensolutions appears in the pendulum solution (Pendellosung). In a magnetically ordered crystal the pendulum solution in the general case (as a result of the nonorthogonality of the eigenpolarizations) gives six periods of beating of the intensity of the primary and secondary waves with the thickness of the crystal, in contrast to the two periods observed for x rays.

The general structure of the solution of the diffraction problem in the case discussed is also presented by Eq. (4.4). In order to find the explicit form of this expansion, it is necessary to specify the boundary conditions. We will assume that the crystal is a plane-parallel plate. As in the case of an unsplit line, using the relation between k_1 and k_2, Eqs. (4.8) and (4.9), imposed by the boundary conditions, from Eq. (4.3) we will uniquely determine all parameters of the four eigenwaves excited in the crystal for a given angle of incidence of the primary wave on the crystal surface. The four values of the parameter ϵ_1 which determine the wave vectors of the eigensolutions are given by the roots of the equation

$$\det\left[\varepsilon-\frac{1}{2}\hat{b}(\hat{F}-\hat{\delta})\right]=0, \qquad (4.21)$$

where the four-row matrices $\hat{b}$ and $\hat{\delta}$ are expressed in terms of the parameters b and δ (see Eq. (4.10) by the relations: $b_{ik} = \delta_{ik}$ if $i \le 2$, $b_{ik} = b\delta_{ik}$ if $i > 2$, $(\hat{\delta})_{ik} \equiv 0$ if $i \le 2$, and $(\hat{\delta})_{ik} = \delta\delta_{ik}$ if $i > 2$.

For what follows it is convenient to assume that the eigensolutions in expansion (4.4) are normalized by the condition $|E_1^p| = 1$ and represented in the form

$$\mathbf{E}_1^p=\mathbf{n}_p=a_{1p}\chi_1+a_{2p}\chi_2,\quad \mathbf{E}_2^p=B_p\mathbf{n}_p'=a_{3p}\chi_1'+a_{4p}\chi_p',$$
$$B_p=\frac{|E_2^p|}{|E_1^p|}=\sqrt{|a_{3p}|^2+|a_{4p}|^2}, \qquad (4.22)$$

where χ_i and χ_i' are the polarization basis vectors (for directions 1 and 2, respectively) in which the matrix $\hat{F}$ is written. The quantities a_{ip} are expressed in terms

of the matrix elements $\hat{F}$, the eigenvalue of Eq. (4.21) ϵ_p, and the parameters δ and b by the relation

$$a_{ip} = CD(\varepsilon_p)_{ki}, \quad \hat{d}(\varepsilon_p) = \varepsilon_p \hat{E} - \frac{1}{2}\hat{b}(\hat{F} - \hat{\delta}), \tag{4.23}$$

where D_{ki} is the cofactor of the element d_{ki} of the matrix $\hat{d}(\epsilon_p)$ defined in Eq. (4.23), and C is a normalization coefficient. Consequently, the coefficients for expansion of the amplitudes of the field in the eigensolution in the polarization basis vectors are expressed in terms of the cofactors to the elements of any row of the matrix $\hat{d}(\epsilon_p)$. For definiteness we will assume below that they are expressed in terms of the cofactors to the first row. Representing the eigenpolarization vectors in the generally accepted form:

$$\begin{aligned} \mathbf{n}_p &= (\cos\alpha_p \chi_2 + e^{i\beta_p}\sin\alpha_p \chi_1)\, e^{i\eta_p}, \\ \mathbf{n}'_p &= (\cos\alpha'_p \chi'_2 + e^{i\beta'_p}\sin\alpha'_p \chi'_1)\, e^{i\eta'_p}, \end{aligned} \tag{4.24}$$

we obtain the following expressions for the parameters α, β, and η:

$$\begin{aligned} &\cos\alpha_p = |a_{1p}|, \quad e^{i\eta_p} = \frac{a_{2p}}{|a_{2p}|}, \quad \operatorname{tg}\alpha_p e^{i\beta_p} = \frac{a_{1p}}{a_{2p}}, \\ &\cos\alpha'_p = |a_{4p}|, \quad e^{i\eta'_p} = \frac{a_{4p}}{|a_{4p}|}, \quad \operatorname{tg}\alpha'_p e^{i\beta'_p} = \frac{a_{3p}}{a_{4p}}. \end{aligned} \tag{4.25}$$

The polarization properties of the eigenwaves, the values of B_p, and their dependence on the parameter δ (the angle of incidence) determine all the features and polarization dependences of diffraction in magnetically ordered crystals. In particular, far from the Bragg condition (large $|\delta|$) it follows from (4.22)–(4.23) that the amplitude of the secondary wave approaches zero, and the eigenpolarizations $\mathbf{n}_p$, as should be the case, coincide with the eigenpolarizations for direct traversal.[58]

f) Solution of the boundary-value problem. If a wave whose polarization vector is $\mathbf{e} = \cos\alpha\chi_2 + e^{i\beta}\sin\alpha\chi_1$ is incident on a crystal, then in the Laue case ($b > 1$) we find for the intensity of the radiation which has passed through the crystal in the primary and secondary directions, from Eq. (4.4) and utilizing the boundary conditions (4.12),[82]

$$\begin{aligned} I_t(\mathbf{e}) &= \sum_{p=1}^{4} |C_p(\mathbf{e})|^2 |\gamma_p|^2 + 2\,\mathrm{Re}\sum_{p>k} C_p(\mathbf{e})\, C_k^*(\mathbf{e})\, \gamma_p \gamma_k^* (\mathbf{n}_p \mathbf{n}_k^*), \\ I_R(\mathbf{e}) &= \sum_{p=1}^{4} |C_p(\mathbf{e})|^2 |\gamma_p|^2 B_p^2 + 2\,\mathrm{Re}\sum_{p>k} C_p(\mathbf{e})\, C_k^*(\mathbf{e})\, B_p B_k \gamma_p \gamma_k^* (\mathbf{n}'_p \mathbf{n}'^*_k), \end{aligned} \tag{4.26}$$

where $C_p(\mathbf{e}) = \Delta_{Lp}(\mathbf{e})/\Delta_L$, Δ_L is the determinant of the matrix a_{ik} (see Eq. (4.23)), $\Delta_{Lp}(\mathbf{e})$ is the determinant obtained from Δ_L if in its p-th column we set $a_{1p} = e^{i\beta}\sin\alpha$, $a_{2p} = \cos\alpha$, $a_{3p} = a_{4p} = 0$; $\gamma_p = \exp(i\epsilon_p \kappa L/2\cos(\kappa s))$; L is the crystal thickness.

The polarization vectors of the radiation which has passed through the crystal are determined by the relations

$$\mathbf{n}_t(\mathbf{e}) = \frac{\sum_p C_p(\mathbf{e})\,\gamma_p \mathbf{n}_p}{\left|\sum_p C_p(\mathbf{e})\,\gamma_p \mathbf{n}_p\right|}, \quad \mathbf{n}_R(\mathbf{e}) = \frac{\sum_p C_p(\mathbf{e}) B_p \gamma_p \mathbf{n}'_p}{\left|\sum_p C_p(\mathbf{e})\, B_p \gamma_p \mathbf{n}'_p\right|}. \tag{4.27}$$

As follows from Eqs. (4.26) and (4.27), the intensities and polarizations of the radiation in the primary and secondary directions undergo beats with the crystal thickness, the Pendellosung effect. In contrast to x rays, for which there are two beat periods, in Mossbauer diffraction, as a result of the nonorthogonality of the eigenpolarizations, in the general case it is possible for six beat periods to occur, on the basis of the number of different values of the quantities $\epsilon_p - \epsilon_{p'}$, $p \neq p'$, which determine the beat periods. For a fixed crystal thickness, beats appear for a change in the γ-ray energy as a result of the dependence of the amplitudes and consequently also the differences $\epsilon_p - \epsilon_{p'}$ on energy. As follows from Eq. (4.26), the eigenwaves, which correspond to the zero roots of Eq. (4.21), are propagated through the crystal without damping, i.e., for the eigenwaves there is a complete suppression of inelastic channels. In the case of resolved hyperfine structure of the Mössbauer spectrum, neglecting Rayleigh scattering, the complete suppression effect can be realized for two eigensolutions,[79] i.e., absorption can be absent for radiation of any polarization. However, as a result of the fact that in reality there is always an interaction of the γ rays with electrons, a complete suppression of inelastic processes is never achieved, and a small but finite absorption can occur, of the same order as the anomalous absorption of x rays.

In the case of an unpolarized primary beam, we obtain for the intensities of radiation which has passed through the crystal, from Eq. (4.26),

$$\begin{aligned} I_t &= \frac{1}{2|\Delta_L|^2}\Big[\sum_{\substack{p \\ i=1,2}} |\Delta^i_{Lp}|^2 |\gamma_p|^2 + 2\,\mathrm{Re}\sum_{\substack{p>k, \\ i=1,2}} \Delta^i_{Lp}\Delta^{i*}_{Lk}\gamma_p\gamma_k^*(\mathbf{n}_p\mathbf{n}_k^*)\Big], \\ I_R &= \\ &\frac{1}{2|\Delta_L|^2}\Big[\sum_{\substack{p \\ i=1,2}} |\Delta^i_{Lp}|\,|B_p^2|\,|\gamma_p|^2 + 2\,\mathrm{Re}\sum_{\substack{p>k, \\ i=1,2}} \Delta^i_{Lp}\Delta^{i*}_{Lk} B_p B_k \gamma_p \gamma_k^* (\mathbf{n}'_p \mathbf{n}'^*_k)\Big], \end{aligned} \tag{4.28}$$

where $\Delta^1_{Lp} \equiv \Delta_{Lp}$ for $\alpha = 0$, $\Delta^2_{Lp} \equiv \Delta_{Lp}$ for $\alpha = \pi/2$, $\beta = 0$.

Beams which have passed through the crystal turn out to be partially polarized and are described by the following polarization density matrices:

$$\begin{aligned} \rho_t &= \frac{1}{I_t}\sum_{s=1,2} I_t(\chi_s)\,\rho(\mathbf{n}_t(\chi_s)), \\ \rho_R &= \frac{1}{I_R}\sum_{s=1,2} I_R(\chi_s)\,\rho(\mathbf{n}_R(\chi_s)), \end{aligned} \tag{4.29}$$

where $\rho(\mathbf{e})$ is defined in Eq. (3.9).

Equations (4.26)–(4.29) assume that the angle of incidence and energy of the primary beam are strictly fixed. In a real situation the primary beam has a finite angular and energy width and detection of the secondary beams is accomplished with finite angular and energy resolution. Therefore the observed quantities are described by expressions obtained from Eqs. (4.26)–(4.29) by means of appropriate averaging. Thus, in a typical experimental situation with an angular divergence of the primary beam and angular size of the detector significantly exceeding the angular size of the region of diffraction reflection, the observed quantities turn out to be those obtained from Eqs. (4.26)–(4.29) by integration over the parameter δ. Integration over δ of the expressions (4.27) leads to the result that, even for a completely polarized primary beam, the result of polarization measurements is described by the polarization matrix corresponding to a partially polarized beam:

$$\bar{\rho}_t(\mathbf{e}) = \frac{\int I_t(\mathbf{e}, \delta)\,\rho(\mathbf{n}_t(\mathbf{e}, \delta))\,d\delta}{\int I_t(\mathbf{e}, \delta)\,d\delta}, \quad \bar{\rho}_R(\mathbf{e}) = \frac{\int I_R(\mathbf{e}, \delta)\,\rho(\mathbf{n}_R(\mathbf{e}, \delta))\,d\delta}{\int I_R(\mathbf{e}, \delta)\,d\delta}. \tag{4.30}$$

In a similar way (see Eq. (3.14)) averaging is carried out over energy with inclusion of the line shape of the primary beam, the scatterer, and if necessary the detector (for a resonance detector).

In the Bragg case ($b < 0$) for the coefficients C_p in the expansion (4.4), using the boundary conditions (4.13), we find

$$C_p(\mathbf{e}) = \frac{\Delta_{Bp}(\mathbf{e})}{\Delta_B}, \quad \Delta_B = \det \begin{vmatrix} a_{11} & a_{12} & a_{13} & a_{14} \\ a_{21} & a_{22} & a_{23} & a_{24} \\ \gamma_1 a_{31} & \gamma_2 a_{32} & \gamma_3 a_{33} & \gamma_4 a_{34} \\ \gamma_1 a_{41} & \gamma_2 a_{42} & \gamma_3 a_{43} & \gamma_4 a_{44} \end{vmatrix}. \quad (4.31)$$

The determinant $\Delta_{Bp}(\mathbf{e})$ is obtained from Δ_B in the same way as $\Delta_{Lp}(\mathbf{e})$ is obtained from Δ_L (see Eq. (4.26)), and the remaining designations in Eq. (4.31) are the same as above.

The intensity and polarization of the radiation which has passed through the crystal $I_t(\mathbf{e})$ and $n_t(\mathbf{e})$, as before, are determined by the first relations in Eqs. (4.26)–(4.30), but with coefficients C_p determined by Eq. (4.31). The determinants Δ^i_{Bp} now entering into Eq. (4.28) are related to Δ_{Bp} in the same way as Δ^1_{Lp} is related to Δ_{Lp}.

The corresponding quantities for radiation reflected from a crystal are described by the expressions

$$I_R(\mathbf{e}) = \sum_p |C_p(\mathbf{e})|^2 B_p^2 + 2\,\mathrm{Re} \sum_{p>k} C_p(\mathbf{e}) C_k^*(\mathbf{e}) B_p B_k (\mathbf{n}'_p \mathbf{n}'^*), \quad (4.32)$$

$$n_R(\mathbf{e}) = \frac{\sum_p C_p(\mathbf{e}) B_p \mathbf{n}'_p}{\left|\sum_p C_p(\mathbf{e}) B_p \mathbf{n}'_p\right|}, \quad (4.33)$$

$$I_R = \frac{1}{2|\Delta_B|^2}\left[\sum_{\substack{p \\ i=1,2}} |\Delta^i_{Bp}|^2 B_i^2 + 2\,\mathrm{Re} \sum_{\substack{p>k \\ i=1,2}} \Delta^i_{Bp} \Delta^{i*}_{Bk} B_p B_k (\mathbf{n}'_p \mathbf{n}'^*_k)\right]. \quad (4.34)$$

Exactly as in the Laue case, the intensities and polarizations of beams which have passed through the crystal and which have been reflected undergo beats with change of crystal thickness and γ-ray energy. However, the beam amplitude is damped with crystal thickness much more rapidly than in the Laue geometry, since in the Bragg case the imaginary additions to the wave vectors in the crystal, generally speaking, turn out to be large. The integral characteristics are described by expressions completely similar to Eqs. (3.14), (4.18), and (4.30).

g) Diffraction reflection from thick crystals. The formulas given above are valid for arbitrary crystal thickness. In the limiting cases they are substantially simplified. In the case of thin crystals $\mathrm{Im}\,\mathbf{k}^p_i \mathbf{s} L \ll 1$ (p = 1, 2, 3, 4) Eqs. (4.32)–(4.34) go over, for example, to the expressions of the kinematic theory. For thick crystals $\mathrm{Im}\,\mathbf{k}^p_i \mathbf{s} L \gg 1$ in the Bragg case, of the four eigenwaves in the crystal, only two are excited, which have maximum damping. The contribution of the two other eigenwaves to the solution (4.4) turns out to be exponentially small. Assuming that the maximum damping occurs for the eigensolutions 1 and 2, for coefficients C_p which have no smallness, we obtain from Eq. (4.31) the expressions

$$C_1(\mathbf{e}) = \frac{e^{i\beta}\sin\alpha a_{22} - \cos\alpha a_{12}}{a_{11}a_{22} - a_{21}a_{12}}, \qquad C_2(\mathbf{e}) = \frac{\cos\alpha a_{11} - e^{i\beta}\sin\alpha a_{21}}{a_{11}a_{22} - a_{21}a_{12}}. \quad (4.35)$$

which are identical with the expansion coefficients of the incident wave amplitude in the basis vectors of the eigenpolarizations $\mathbf{n}_1$ and $\mathbf{n}_2$. In this case the reflection curves of waves whose polarizations coincide with the eigenpolarizations are described by the angular dependence of the quantities B_1 and B_2. Here it is necessary to have in mind that, generally speaking, the eigenpolarizations change along the reflection curve. Since in the general case the eigenpolarizations $\mathbf{n}'_1$ and $\mathbf{n}'_2$ are not orthogonal, the reflection curve for unpolarized radiation is not simply one half the sum of the curves for $\mathbf{n}'_1$ and $\mathbf{n}'_2$, but contains also an interference addition. Here the reflection coefficient takes the form

$$R = \frac{1}{2}(1 - |\mathbf{n}_1\mathbf{n}_2^*|^2)^{-1}[B_1^2 + B_2^2 - 2\,\mathrm{Re}\,(\mathbf{n}'_1\mathbf{n}'^*_2)(\mathbf{n}_1^*\mathbf{n}_2) B_1 B_2]. \quad (4.36)$$

The polarization density matrix of the scattered radiation is described by the expression

$$\bar{\rho} = A\{B_1^2 \rho(\mathbf{n}'_1) + B_2^2 \rho(\mathbf{n}'_2) - B_1 B_2 [(\mathbf{n}_1^* \mathbf{n}_2)\rho(12) + (\mathbf{n}_2^* \mathbf{n}_1)\rho(21)]\}, \quad (4.37)$$

where the matrices $\rho(ik)$ are given by the relations $\rho(ik)_{pq} = (\mathbf{n}'_i)_p (\mathbf{n}'^*_k)_q$; A is a normalization factor. The matrix (4.37) corresponds to a degree of polarization of the scattered radiation

$$P = \frac{2\sqrt{(f^-)^2 + |D|^2}}{B_1^2 + B_2^2 - 2B_1 B_2\,\mathrm{Re}\,[(\mathbf{n}_1^*\mathbf{n}_2)(\mathbf{n}_1\mathbf{n}_2'^*)]}. \quad (4.38)$$

The vector of a polarization partially represented in the scattered radiation in the basis vectors χ'_1 and χ'_2 (see Eq. (4.24)) is determined by parameters α and β which satisfy the relation

$$\mathrm{tg}\,\alpha e^{i\beta} = \frac{D}{\sqrt{(f^-)^2 + |D|^2} - f^-}, \quad (4.39)$$

where

$$f^- = \frac{1}{2}\{B_1^2(|n'_{11}|^2 - |n'_{12}|^2) + B_2^2(|n'_{21}|^2 - |n'_{22}|^2) - 2B_1B_2\,\mathrm{Re}\,(\mathbf{n}_1^*\mathbf{n}_2)[n'_{11}n'^*_{21} - n'_{12}n'^*_{22}]\},$$

$$D = B_1^2 n'_{11}n'^*_{12} + B_2^2 n'_{21}n'^*_{22} - B_1B_2[(\mathbf{n}_1^*\mathbf{n}_2)n'_{11}n'^*_{22} + (\mathbf{n}_2^*\mathbf{n}_1)n'_{21}n'^*_{12}],$$

and $\mathbf{n}_{pe}$ is the projection of the vector $\mathbf{n}_p$ on the e-th polarization basis vector. From Eqs. (4.36) and (4.37), as in the previous section, it is possible to obtain characteristics which are integral in the angle of incidence and energy of the γ rays.

Using expressions (4.35)–(4.39), we can analyze the general nature of the dependence of the reflected radiation intensity and its polarization on small changes in the angle of incidence near the Bragg condition.[82] For definiteness we will assume below that the symmetric Bragg case is realized. It is convenient at first to consider the case of the Hermitian matrix $\hat{F} - \hat{\delta}$, which corresponds to neglect of absorption. In this case from the properties of the solutions of the system (4.3) it follows that the quantity $B_i \equiv 1$ if ϵ_i, the root of the secular equation (4.21), is complex. This means that in the entire region of angles $\Delta\theta$ (or corresponding values of the parameter δ), where all four roots of the secular equation (4.21) are complex, the reflection coefficient of a wave with any polarization goes to unity. In the region of angles where two roots are real and two are complex, the reflection coefficient reaches unity only for an isolated eigenpolarization determined by the solution which is damped in the interior of the crystal. In the region of four real roots the reflection coefficient for a wave with any polarization is less than unity. Large deviation angles from the Bragg condition correspond to four real roots of Eq. (4.21) and a reflection coefficient R approaching zero. Therefore the typical reflection curve of unpolarized radiation has the form shown in Fig. 9. The regions of values of the parameter δ, $\delta_1 < \delta < \delta_2$, $\delta_5 < \delta < \delta_6$, cor-

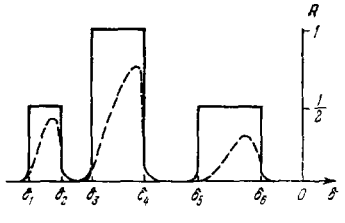

FIG. 9. Appearance of reflection curve of an unpolarized beam for a perfect magnetically ordered crystal in the absence of absorption (solid curve) and with inclusion of absorption (dashed curve). In the absence of absorption the angular intervals for which $\delta_1 < \delta < \delta_2$, $\delta_5 < \delta < \delta_6$ correspond to selective reflection of one of the eigenpolarizations, and the interval $\delta_4 < \delta < \delta_5$ corresponds to total reflection of any polarization.

respond to two real and two complex roots of the secular equation. In these regions the reflection coefficient is $R \cong 1/2$. The reflected radiation is completely polarized, its polarization vector coinciding with the polarization vector determined by the second relation in (4.24) for the eigensolution which is damped in the interior of the crystal. In the region $\delta_3 < \delta < \delta_4$ we have $R = 1$, and the reflected radiation is unpolarized. In Fig. 9 we have shown a typical situation in which the region of total reflection of any polarization is separated from the regions of selective reflection of polarizations. Depending on the specific form of the matrix $\hat{F}$, the location of the regions of total and selective reflection can vary. In particular, one or both regions of selective reflection can directly adjoin the region of total reflection. The angular size of the region of strong reflection $(\delta_6 - \delta_1)$ depends not only on the values of the scattering amplitudes at the angle, but also on the values of the scattering amplitudes forward and has the order $\delta_6 - \delta_1 \sim \max\{F_{12}, F_{11}^{ps} - F_{22}^{q'}\}$.

On taking into account absorption, the general three-humped nature of the reflection curve is preserved. However, everywhere, except perhaps for individual points, the reflection coefficient turns out to be smaller than in the absence of absorption (in Fig. 9 its qualitative behavior is shown by the dotted line).

The formulas of the present and two preceding sections in the general case solve the problem of diffraction not only for magnetic hyperfine splitting of the Mössbuaer line in the crystal, but in fact also for quadrupole and combined hyperfine splitting. (Indeed, the explicit form of the operator $\hat{F}$ has nowhere been used.) However, analysis of the expressions obtained in the general case is difficult, in particular, because it is not possible to find the roots of Eq. (4.21) in explicit form. As a result, we will analyze below the qualitative features of diffraction in magnetically ordered crystals for a number of cases which permit analytic solution of the diffraction problem.

h) Examples of analytic solution of the dynamical system. 1) Polarization-independent scattering amplitude at zero angle. If the directions $\mathbf{k}_1$ and $\mathbf{k}_2$ coincide with crystallographic axes of high symmetry, for example, with rotation axes of third or higher order, the scattering amplitude at zero angle in these directions turns out to be independent of the polarization, the polarization of a wave scattered at zero angle coinciding with its initial polarization. In other words, for direct passage of a wave in directions of high symmetry, any polarization is an eigenpolarization. In the case discussed the eigenpolarizations of the solutions of the system (4.3) are determined only by the amplitudes for scattering from direction 1 to direction 2 and from direction 2 to direction 1 and are easily found from the form of these amplitudes. Indeed, for a polarization-independent forward-scattering amplitude the system of four scalar equations (4.3) is broken down into two independent systems of two equations if we use as polarization vectors the basis vectors which simultaneously diagonalize the operators $\hat{F}_{12}$ and $\hat{F}_{21}$. Thus, the search for eigenpolarizations reduces to the simultaneous diagonalization of the two second-order matrices which describe 12 and 21 scattering. The matrices

$$\hat{F}_{ik} = \begin{pmatrix} F_{ik}^{11} & F_{ik}^{12} \\ F_{ik}^{21} & F_{ik}^{22} \end{pmatrix}$$

(see Eq. (4.5)) are diagonalized in the polarization basis vectors defined by the relations

$$\mathbf{n} = \frac{\hat{S}\mathbf{n}}{|\hat{S}\mathbf{n}|}, \quad \mathbf{n}' = \frac{\hat{S}'\mathbf{n}'}{|\hat{S}'\mathbf{n}'|}, \text{ where } \hat{S} = \hat{F}_{12}\hat{F}_{21} \quad \hat{S}' = \hat{F}_{21}\hat{F}_{12}. \qquad (4.40)$$

From Eq. (4.40) we obtain, for example, the following expression for the eigenpolarization vector n in terms of the initial basis vectors:

$$\mathbf{n}_{1,2} = [|S_{12}|^2 + |\xi_{1,2} - S_{11}|^2]^{-1/2}[S_{12}\chi_1 + (\xi_{1,2} - S_{11})\chi_2], \qquad (4.41)$$

where

$$\xi_{1,2} = \frac{S_{11}+S_{22}}{2} \pm \sqrt{\left(\frac{S_{11}+S_{22}}{2}\right)^2 + S_{12}S_{21} - S_{11}S_{22}}.$$

The further solution of the diffraction problem is carried out in the same way as in the case of an unsplit line. We note that in the general case the matrix $\hat{S}$ is not Hermitian, and therefore the eigenpolarization vectors $\mathbf{n}_1$ and $\mathbf{n}_2$ defined by Eq. (4.41) are in general not orthogonal.

In the case considered, as for an unsplit line, the eigenpolarizations remain constant over the region of diffraction reflection. This simplifies analysis of the polarization properties of the radiation. For example, if the eigenpolarizations found are orthogonal, then in the Bragg case for scattering in a thick crystal of unpolarized radiation, the polarization density matrix (4.37), averaged over the region of diffraction reflection, corresponds to radiation partially polarized along the vector $\mathbf{n}_1'$ or $\mathbf{n}_2'$, depending on which of the vectors $\mathbf{n}_1$ and $\mathbf{n}_2$ gives the greater scattering amplitude from direction 1 to direction 2. The degree of polarization P is expressed in terms of the matrix elements $F_{12}^{ii} \equiv F_{12}^{i}$, written in terms of the eigenpolarization basis vectors, by the relation

$$P = \frac{|\,|F_{12}^1|\mathscr{F}^1 - |F_{12}^2|\mathscr{F}^2|\,|}{|F_{12}^1|\mathscr{F}^1 - |\mathscr{F}_{12}^2|\mathscr{F}^2|}, \qquad (4.42)$$

where $\mathscr{F}$ are the same quantities as in Eq. (4.19).

Equation (4.42) differs from the result of the kinematic discussion, in which (see Eq. (3.10)) the radiation is partially polarized along the same vector, but the degree of polarization turns out to be $||F_{12}^1|^2 - |F_{12}^2|^2|/(|F_{12}^1|^2 + |F_{12}^2|^2)$. For nonorthogonal eigenpolarizations, as follows from Eq. (4.37), the vector describing the partial polarization differs from the vectors $\mathbf{n}_1'$ and $\mathbf{n}_2'$. In this case to obtain the integral polarization characteristics it is necessary to use directly expressions (4.37) and (4.38). The system of dynamical equations is solved like that discussed above also in the case where the forward-scattering amplitude depends on the polarization, if the polarization vectors $\mathbf{n}_1$ and $\mathbf{n}_1'$ found from (4.40) coincide with the eigenpolarization vectors for direct transmission. This situation can be realized for special mutual orientations of $\mathbf{k}_1$ and $\mathbf{k}_2$ and for directions characterizing the magnetic structure of the crystal. For the magnetic peaks in an antiferromagnetic crystal, for example, the case considered is realized if the antiferromagnetic axis lies in the plane of $\mathbf{k}_1$ and $\mathbf{k}_2$, perpendicular to this plane, or the difference of the azimuthal angles of the wave vectors $\mathbf{k}_1$ and $\mathbf{k}_2$ relative to the antiferromagnetic axis amounts to $\pi/2$. In the first two cases the π and σ polarizations turn out to be eigenpolarizations. In the latter case, the eigenpolarizations are also linear, but are given by the basis vectors (2.5).

2) The case of a biquadratic secular equation. To find analytic expressions for the eigensolutions of Maxwell's equations and to trace the nature of the change in the polarization properties of the radiation in the diffraction region is possible if the secular equation has biquadratic degeneracy. The case of a biquadratic equation is real-

ized for physically interesting diffraction experiment conditions. For example, if an axis distinguished by magnetic properties (for example, an antiferromagnetic axis) exists in a cubic crystal, and the vectors $\mathbf{k}_1$ and $\mathbf{k}_2$ form identical angles with this axis.

For analysis of this case it is desirable to use as polarization basis vectors in Eq. (4.3) the eigenpolarization basis vectors for direct transmission in directions 1 and 2. In these basis vectors the matrix $\hat{F}$ is simplified, since its elements, which describe scattering at zero angle, take the form

$$\hat{F}_{11}=\begin{pmatrix} F_{11}^1 & 0 \\ 0 & F_{11}^2 \end{pmatrix}, \quad \hat{F}_{22}=\begin{pmatrix} F_{22}^1 & 0 \\ 0 & F_{22}^2 \end{pmatrix}, \quad \text{where } F_{pp}^i \equiv F_{pp}^{ii},$$

and for the diagonal elements the relation $F_{11}^1 - F_{11}^2 = F_{22}^1 - F_{22}^2$ is satisfied. The latter relation is a reflection of the fact that for equivalent directions in the crystal the differences of the refractive indices of the eigenwaves (we have in mind direct transmission) are identical for each of the directions. Here for the symmetric Bragg case ($b = -1$) the condition that the secular equation (4.21) go over to biquadratic form is

$$F_{12}^{12}F_{21}^{21} - F_{21}^{12}F_{12}^{21} = 0. \tag{4.43}$$

If the condition (4.43) is satisfied the eigenvalues and eigensolutions of Eq. (4.21) (see Eq. (4.23)) in the basis vectors coinciding with the eigenpolarization vectors for direct transmission are determined by the formulas:

$$\varepsilon - \frac{1}{4}(F_{11}^{11}+F_{11}^{22}-F_{22}^{11}-F_{22}^{22}) - \frac{\delta}{2} = \tilde{\varepsilon} = \pm\frac{1}{\sqrt{2}}\left\{\frac{\delta^2}{2} - \delta(b_{11}+b_{22}) + (b_{11}^2+b_{22}^2-\Delta_+) \pm \sqrt{(b_{11}-b_{22})^2\left[\delta^2 - 2\delta(b_{11}+b_{22})\left(1+\frac{F_{21}^{22}F_{12}^{21}-F_{12}^{11}F_{21}^{11}}{b_{11}^2-b_{22}^2}\right)\right] + (b_{11}^2+b_{22}^2-\Delta_+)^2 - 4\det\bar{F}}\right\}^{1/2}, \tag{4.44}$$

$$\left.\begin{aligned} a_{1p} &= (\tilde{\varepsilon}_p - a)^{-1}\left[F_{12}^{11}F_{21}^{11}(\tilde{\varepsilon}_p^2 - b^2) + F_{12}^{12}F_{21}^{21}(b+\tilde{\varepsilon}_p)(a+\tilde{\varepsilon}_p) + \Delta_1\Delta_2\right], \\ a_{2p} &= F_{12}^{22}F_{21}^{21}(a+\tilde{\varepsilon}_p) + F_{12}^{21}F_{21}^{11}(b+\tilde{\varepsilon}_p), \quad a_{3p} = F_{21}^{11}(\tilde{\varepsilon}_p^2 - b^2) + F_{12}^{22}\Delta_2, \\ a_{4p} &= -\left[F_{12}^{21}\Delta_2 + F_{21}^{21}(b-\tilde{\varepsilon}_p)(a+\tilde{\varepsilon}_p)\right], \quad B_p = \frac{\sqrt{|a_{3p}|^2+|a_{4p}|^2}}{\sqrt{|a_{1p}|^2+|a_{2p}|^2}}, \end{aligned}\right\} \tag{4.45}$$

where

$$a = \frac{1}{2}(F_{11}^{11}+F_{22}^{11}) - \frac{\delta}{2}, \quad b = \frac{1}{2}(F_{11}^{22}+F_{22}^{22}) - \frac{\delta}{2},$$
$$b_{11} = \frac{1}{2}(F_{11}^{11}+F_{22}^{11}), \quad b_{22} = \frac{1}{2}(F_{11}^{22}+F_{22}^{22}),$$
$$\Delta_1 = F_{12}^{11}F_{12}^{22} - F_{12}^{12}F_{12}^{21}, \quad \Delta_2 = F_{21}^{11}F_{21}^{22} - F_{21}^{12}F_{21}^{21},$$
$$\Delta_+ = F_{12}^{12}F_{21}^{21} + F_{12}^{11}F_{21}^{11} + F_{12}^{22}F_{21}^{22} + F_{21}^{12}F_{12}^{21}.$$

Equations (4.44) and (4.45) completely determine the eigensolutions of the system of dynamical equations. In particular, if the eigenpolarizations for direct transmission are linear and mutually perpendicular, the polarization vector parameters α and β in the eigensolutions are determined by Eq. (4.25). This means that the eigenpolarizations (in the general case elliptical) are characterized by a polarization ellipse whose axis is rotated relative to the initial basis vector χ_1 by some angle φ. The angle $\tilde{\varphi}$ and the ratio of the polarization ellipse axes a_1/a_2 are not constant over the region of diffraction reflection and are determined by the relations:

$$\tilde{\varphi}_p = -\frac{1}{2}\operatorname{arctg} 2\alpha_p, \quad \frac{a_1}{a_2} = \sqrt{\frac{(1+\operatorname{tg}^2\tilde{\varphi}_p)\,|\operatorname{tg}\alpha_p \sin\beta_p|}{(1+\operatorname{tg}\tilde{\varphi}_p \operatorname{tg}\alpha_p)^2}}. \tag{4.46}$$

Under the same conditions for the Laue case, the secular equation reduces to biquadratic for $F_{21}^{22}F_{12}^{22} - F_{12}^{11}F_{21}^{11} = 0$.

3. Completely resolved Zeeman splitting of the Mössbauer line. Analysis of the expressions given in the preceding sections is substantially simplified in case in which Mössbauer scattering occurs through one or two different Zeeman transitions. Here the transitions should be considered different not only in the case when they correspond to different energies, but also for identical Zeeman transition energies in the case of degeneracy of the levels (for example, for quadrupole splitting). If there are several Mössbauer nuclei in the unit cell of the crystal, then transitions in nuclei occupying different positions in the cell also must be considered different retardless of whether or not their energies coincide. For example, in an antiferromagnetic crystal with two magnetic atoms in the unit cell, with a completely resolved Zeeman splitting, each line of the Mössbauer spectrum receives contributions from transitions in nuclei located at the zero of H and $-\mathbf{H}$, i.e., each line corresponds to two different transitions.

Let us consider first the suppression of inelastic channels.[79] For one Zeeman transition in the system (4.3) the matrix elements are given by

$$F_{mn}^{pq} \sim \mathbf{n}_n^*(\mathbf{k}_n)_q \mathbf{n}_m(\mathbf{k}_m)_p e^{i(\mathbf{k}_n - \mathbf{k}_m)\mathbf{r}},$$

where r gives the position of the nucleus, and therefore the columns of the matrix $\hat{F}$ are linearly dependent, since they differ only by a common factor. The consequence of this linear dependence is that in the secular equation (4.21) for $\delta = 0$ the coefficients are different from zero only for ϵ^4, ϵ^3, and the three routes of the secular equation vanish. This means that for $\delta = 0$ there is no damping in the corresponding three eigensolutions, and therefore the complete suppression of inelastic channels is realized. If scattering occurs through two different transitions, each element of the matrix $\hat{F}$ consists of two terms of the same type as above. Here the linear dependence of the columns turns out to be such that for $\gamma = 0$ ϵ^2 is present in the secular equation in addition to ϵ^4 and ϵ^3. This means that two roots vanish and damping is absent in two eigensolutions. If the two zero roots are not due to the fact that γ rays of some polarization interact simply with the nuclei of the crystal, then in this case also for $\delta = 0$ the complete suppression effect occurs, regardless of the multipolarity of the nuclear transition. A similar analysis shows that in the case of three transitions for $\delta = 0$ only one root vanishes and the suppression effect occurs only for a polarization corresponding to the solution with zero eigenvalue. For four transitions the suppression effect is not realized in the general case, i.e., there is no superposition of the waves $\mathbf{E}_1$ and $\mathbf{E}_2$ for which the amplitude for formation of the excited nucleus in the transition discussed vanishes.

So far we have assumed only the existence of hyperfine splitting of the Mössbauer line, without specifying the type of crystalline structure and magnetic structure of the sample. The results presented below are for magnetic diffraction peaks in antiferromagnetic crystals.

For a polarization-independent forward-scattering amplitude we find by means of Eqs. (4.40) and (4.41) that the eigenpolarizations for each of the directions 1 and 2 are linear, orthogonal, and rotated relative to the basis vectors $\chi_1 = [\mathbf{H}\times\mathbf{k}]/|[\mathbf{H}\times\mathbf{k}]|$, $\chi_1^1 = [\mathbf{H}\times\mathbf{k}']/|[\mathbf{H}\times\mathbf{k}']|$ by an angle $\tilde{\varphi}$ determined by the relation

$$\operatorname{tg}\tilde{\varphi} = \frac{\xi_{1,2} - S_{11}}{S_{12}}. \tag{4.47}$$

The matrix $\hat{S}$, with accuracy to a factor unimportant here, is

$$\hat{S}=\begin{pmatrix}\sin^2\alpha_t(1+\cos 2\alpha_t'\cos 2\Phi) & \frac{1}{2}\cos 2\alpha_t'\sin 2\alpha_t\sin 2\Phi\\ \frac{1}{2}\cos 2\alpha_t'\sin 2\alpha_t\sin 2\Phi & \cos^2\alpha_t(1-\cos 2\alpha_t'\cos 2\Phi)\end{pmatrix}. \quad (4.48)$$

The matrix $\hat{S}'$ is obtained from Eq. (4.48) if in it we replace α_t by α_t', α_t' by α_t, and Φ by $-\Phi$. The parameters α_t and α_t' determine $\mathbf{n}_t$ and $\mathbf{n}_t'$, the polarization vectors of the radiation emitted in the transition through which the scattering occurs, in the directions $\mathbf{k}_1$ and $\mathbf{k}_2$; Φ is the phase difference of the phase factors of the polarization vectors $\mathbf{n}_t$ and $\mathbf{n}_t'$ (see Eqs. (2.4) and (2.5)). For example, for a magnetic dipole transition we have

$$\Delta M=\pm 1,\quad \operatorname{tg}\alpha_t=\pm\cos\theta,\quad \operatorname{tg}\alpha_t'=\pm\cos\theta',\quad \Phi=\pm(\varphi-\varphi'),$$

where the designations of the angles are the same as in Eq. (3.16). The eigenvalues of the matrices $\hat{S}$ and $\hat{S}'$ in the case discussed turn out to be identical and equal to

$$\xi=\frac{1}{2}[1-\cos 2\alpha_t\cos 2\alpha_t'\cos 2\Phi \pm\sqrt{(1-\cos 2\alpha_t\cos 2\alpha_t'\cos 2\Phi)^2-\sin^2 2\alpha_t\sin^2 2\alpha_t'}]. \quad (4.49)$$

In the basis vectors coinciding with the eigenpolarization vectors found, the elements of the matrix $\hat{F}$ describing scattering from direction 1 to 2 and the reverse take the form

$$\hat{F}_{12}=-\hat{F}_{21}=ie^{i\varphi_E}\frac{4\pi}{V\kappa^2}\begin{pmatrix}\sqrt{\sigma_{max}} & 0\\ 0 & \sqrt{\sigma_{min}}\end{pmatrix}; \quad (4.50)$$

here φ_E is the phase of the energy factor in the Mössbauer amplitude (2.11), and σ_{max} and σ_{min} are the maximum and minimum cross sections for scattering for the unit cell from direction 1 to 2 and the reverse, which are achieved precisely for the eigenpolarizations found. Further solution of the diffraction problem for each of the two sets of eigenpolarizations found is described by the formulas of Sec. b of Chap. 4, in which the quantities F_{12} and F_{21} must be considered to be defined by Eq. (4.50). The expressions found above for the eigenpolarizations in the case of a polarization-independent forward-scattering amplitude for scattering through an isolated Zeeman transition turn out to be valid also for an arbitrary value of the Zeeman splitting. In this case the amplitudes F_{12}^1 and, as a consequence, the integral scattering characteristics (4.42), turn out to be dependent on the magnitude of the Zeeman splitting.

Let us now consider the situation in which the forward-scattering amplitude depends on the polarization, but the secular equation reduces to biquadratic. As already noted, this situation is realized in the symmetric Bragg case if the wave vectors $\mathbf{k}_1$ and $\mathbf{k}_2$ form identical angles with the antiferromagnetic axis. In this case $\hat{F}^N$ in the polarization basis vectors (2.5) for a dipole transition with $\Delta M = \pm 1$ in the nuclear diffraction peaks is given by the expressions

$$\hat{F}_{11}=\hat{F}_{22}=A\begin{pmatrix}\sin^2\alpha_t & 0\\ 0 & \cos^2\alpha_t\end{pmatrix},$$
$$\frac{1}{A}\hat{F}_{12}=\left(\frac{1}{A}\hat{F}_{21}\right)^*=\frac{2\tilde{F}_H^N}{N}\begin{pmatrix}i\sin^2\alpha_t\sin\Phi & i\sin\alpha_t\cos\alpha_t\cos\Phi\\ -i\sin\alpha_t\cos\alpha_t\cos\Phi & i\cos^2\alpha_t\sin\Phi\end{pmatrix}, \quad (4.51)$$

where $A=(4\pi/V\kappa^2)Nf_{coh}^0$ and f_{coh}^0 is determined by Eq. (2.8) if in it we omit the factor $(\mathbf{en}^*_{mm'}(\mathbf{k}))(\mathbf{n}_{mm'}(\mathbf{k}')\mathbf{e}')$, $\hat{F}_H^N$ is the same quantity as in Eqs. (3.17), N is the number of Mössbauer nuclei in the unit cell and the remaining designations are the same as in Eq. (4.48). Here the secular equation (4.21) turns out to be biquadratic and, using Eq. (4.44), we obtain for its roots:

$$\tilde{\varepsilon}=\pm\frac{1}{\sqrt{2}}\left\{\frac{\tilde{\delta}^2}{2}-\tilde{\delta}+B(\alpha_t,\tilde{F}_H^N)\pm\left[\cos^2 2\alpha\left(\tilde{\delta}^2-2\tilde{\delta}\left(1-\left|\frac{2\tilde{F}_H^N}{N}\right|^2\sin^2\Phi\right)\right)+B(\alpha_t\tilde{F}_H^N)^2-\frac{1}{4}\sin^4 2\alpha_t\left(1-\left|\frac{2\tilde{F}_H^N}{N}\right|^2\right)^2\right]^{1/2}\right\}^{1/2}, \quad (4.52)$$

where

$$\tilde{\varepsilon}=\frac{1}{A}\left(\varepsilon-\frac{\delta}{2}\right),\quad \tilde{\delta}=\frac{\delta}{A},$$
$$B(\alpha_t\tilde{F}_H^N)=\cos^4\alpha_t+\sin^4\alpha_t-2\left|\frac{\tilde{F}_H^N}{N}\right|^2(1-\cos^2 2\alpha_t\cos 2\Phi).$$

The quantities a_{ip} corresponding to the p-th root found are defined by the following relations:

$$\left.\begin{aligned}
a_{1p}&=\left|\frac{2\tilde{F}_H^N}{N}\right|^2\left(\sin^2\alpha_t-\frac{\tilde{\delta}}{2}-\tilde{\varepsilon}_p\right)^{-1}\sin^2\alpha_t\left[\left(\frac{\tilde{\delta}^2}{4}-\tilde{\delta}\cos 2\alpha_t-\tilde{\varepsilon}_p\right)\times\sin^2\alpha_t\sin\Phi+\left(\frac{\tilde{\delta}^2}{4}-\frac{\tilde{\delta}}{2}+\tilde{\varepsilon}_p\cos 2\alpha_t-\tilde{\varepsilon}_p^2\right)\cos^2\alpha_t\cos^2\Phi\right.\\
&\qquad\left.+\sin^2\alpha_t\cos^4\alpha_t\left(1-\left|\frac{2\tilde{F}_H^N}{N}\right|^2\right)\right],\\
a_{2p}&=\frac{1}{8}\left|\frac{2\tilde{F}_H^N}{N}\right|^2\sin 4\alpha_t\sin 2\Phi,\\
a_{3p}&=i\sin^2\alpha_t\sin\Phi\left(\frac{2\tilde{F}_H^N}{N}\right)\left[\frac{\tilde{\delta}^2}{4}-\tilde{\delta}\cos^2\alpha_t-\tilde{\varepsilon}_p^2+\right.\\
&\qquad\left.+\cos^4\alpha_t\left(1-\left|\frac{2\tilde{F}_H^N}{N}\right|^2\right)\right],\\
a_{4p}&=\frac{i}{2}\sin 2\alpha_t\cos\Phi\left(\frac{2\tilde{F}_H^N}{N}\right)\left[\frac{\tilde{\delta}^2}{4}-\frac{\tilde{\delta}}{2}+\right.\\
&\qquad\left.+\frac{1}{4}\sin^2 2\alpha_t\left(1-\left|\frac{2\tilde{F}_H^N}{N}\right|^2\right)+\tilde{\varepsilon}_p\cos 2\alpha_t-\tilde{\varepsilon}_p^2\right].
\end{aligned}\right\} \quad (4.53)$$

Equations (4.52) and (4.53) describe the dependence of the intensity and polarization characteristics of scattering in the nuclear diffraction peaks on the structure of the antiferromagnetic crystal, the γ-ray energy, and the deviation of the scattering angle from the Bragg condition. For example, for large energy differences from the exact resonance, where the quantity A can be considered real with high accuracy, the eigenpolarizations turn out to be linear. Here the angle formed by the plane of polarization with the polarization basis vectors (2.5) depends on the parameter δ (the deviation from the Bragg angle), and the explicit form of this dependence turns out to be related to the structure of the antiferromagnetic crystal through the quantity $|2\tilde{F}_H^N/N|$. The form of the reflection curve of unpolarized radiation depends on the structure of the antiferromagnetic crystal and the difference of the γ ray energy from the resonance value. For example, for the case $|2\tilde{F}_H^N/N| = 1$, which is realized, in particular, for antiferromagnetic crystals with two magnetic atoms in the unit cell, for large energy detuning and $\cos^2\alpha_t\cos^2\Phi > 1/2$, the characteristic points on the reflection curve (see Fig. 9) are determined by the following value of the parameter $\delta : \delta_1 = \delta_2 = 0$,

$$\delta_3=\cos^2\Phi(1-\sin 2\alpha_t),\ \operatorname{Re}A\quad \delta_4=\cos^2\Phi(1+\sin 2\alpha_t)\operatorname{Re}A,$$
$$\delta_5=2(1-\cos 2\alpha_t\sin\Phi)\operatorname{Re}A,\quad \delta_6=2(1+\cos 2\alpha_t\sin\Phi)\operatorname{Re}A.$$

On the basis of the formulas presented and the results of the preceding sections, it is possible to find the dependence on the details of the magnetic structure of the antiferromagnetic crystal of the integrated reflection coefficient and the corresponding polarization density matrix. Here we will not give the explicit form of these expressions in view of their cumbersome nature.

In the above we have not taken into account Rayleigh scattering. For the nuclear peaks, Rayleigh scattering contributes only to the forward-scattering amplitude, and therefore does not affect the polarization charac-

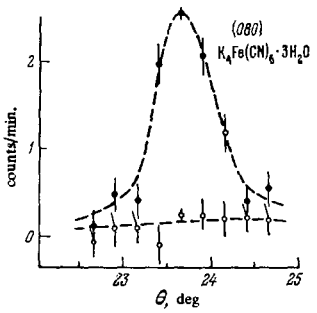

FIG. 10. Diffraction peak due to pure nuclear resonance scattering in an enriched single crystal of $K_4Fe(CN)_6 \cdot 3H_2O$ under conditions of extinction of Rayleigh scattering. [18] The lower curve is the angular dependence of the scattering intensity off-resonance, and the upper curve is the same dependence for coincidence of the γ-ray energy with the resonance value.

teristics of the scattering, but simply shifts the reflection curve as a whole (see Fig. 9) along the abscissa by an amount F_{11}^R.

5. RESULTS OF EXPERIMENTAL RESEARCH

a) Interference of nuclear and Rayleigh scattering. The experimental study of Mössbauer diffraction began with establishment of the coherence of nuclear resonance scattering and Rayleigh scattering, i.e., the existence of interference between these two scattering processes. In the first studies of the Birmingham group[3, 4] the interference of nuclear and Rayleigh scattering was observed in polycrystalline samples of iron with the natural content of the Mössbauer isotope Fe^{57}. These same experiments showed that, as a result of the low activity of the Mössbauer sources and the small natural content of the Mössbauer isotope, it is desirable, in order to obtain quantitative information in a reasonable duration of the experiment, to use single-crystal scatterers enriched in the Mössbauer isotope. In subsequent work of the Birmingham group, carried out in single crystals containing Fe^{57}, for 14.4-keV Mössbauer radiation the interference phenomena (a weak dependence of the intensity of the diffracted radiation on the γ-ray energy) appeared already more distinctly,[16] but as before the results had a qualitative nature (see Fig. 1). Diffraction was also observed under conditions of pure nuclear resonance scattering for a reflection whose Rayleigh structure factor is zero (Fig. 10),[18] and it was shown experimentally[17] that the thermal factor in coherent nuclear resonance scattering is the product of two Lamb-Mössbauer factors (see Eq. (2.11), i.e., does not coincide with the ordinary Debye-Waller factor and does not depend on the scattering angle.

Voĭtovetskiĭ's group has carried out experimental studies of Mössbauer diffraction, utilizing[30-35] the 23.8-keV radiation of the isotope Sn^{119}. This group carried out the first quantitative experimental studies of interference of nuclear and Rayleigh scattering.[32] Use of perfect single crystals of tin as scatterers permitted not only observation of interference of nuclear and Rayleigh scattering, but also observation of dynamic effects in diffraction in the enriched isotope Sn^{119} and in unenriched samples (see below). It was shown[35] that scattering at large angles (high orders of reflection) can be used to separate pure nuclear coherent scattering. The energy dependence observed in ref. 35 of the intensity of the diffraction peak at a scattering angle of 126° is similar to that shown in Fig. 10 and indicates the almost complete absence of coherent Rayleigh scattering under the experimental conditions. The suppression of Rayleigh scattering is due to the fact that the thermal factor in nuclear scattering does not depend on the scattering angle, and the Debye-Waller factor, which enters into the coherent Rayleigh scattering amplitude, falls off rapidly with increasing scattering angle.

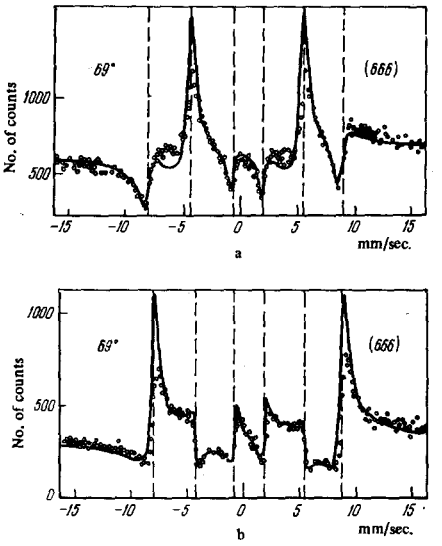

FIG. 11. Interference of nuclear and Rayleigh scattering in Bragg reflection (666) for hematite under conditions of Zeeman splitting of the Mössbauer line. [84] The antiferromagnetic axis is perpendicular to the scattering plane (a) and lies in the scattering plane (b).

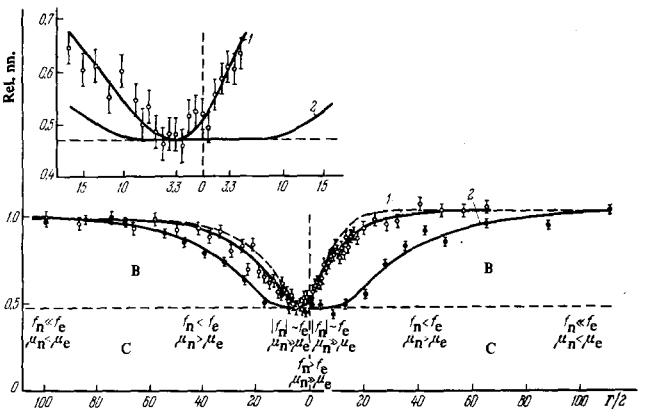

FIG. 12. Dependence of intensity of diffracted beam in Laue diffraction in an enriched single crystal of tin (1) and after transmission through the crystal at an angle different from the Bragg angle (2), as a function of the relative velocity of the source and the crystal. [34]

We have presented above the results of experimental study of the interference of nuclear and Rayleigh scattering in the absence of hyperfine splitting of the Mössbauer line in the scattering crystal. A detailed study of the interference of nuclear and Rayleigh scattering under conditions of hyperfine splitting of the Mössbauer lines in diffraction in a hematite single crystal enriched in the isotope Fe^{57} has been carried out by Artem'ev and co-workers[83, 84]. The interference pattern in the presence of hyperfine fields in the Mössbauer nuclei in the scattering crystal turns out to be much more complex and varied. The sign of the interference term in the intensity of the diffraction peak turns out to depend not only on the sign of the energy difference of the γ-ray and resonance energy, but also on the orientation of the hyperfine fields in the crystal. Figure 11 illustrates the nature of the interference curves and their dependence on the orientation of the magnetic fields in Fe nuclei in hematite. Under the conditions of hyperfine splitting, as follows from the expressions for the coherent amplitude (see Chap. 2), in addition to the interference of nuclear and Rayleigh scattering there is also interfer-

ence of nuclear scattering through different sublevels of the ground and excited states of the Mössbauer nucleus. This interference and its dependence on the orientation of the hyperfine fields were observed for the first time for magnetic reflections in Bragg scattering in hematite.[85]

b) **Anomalous transmission of Mössbauer radiation through crystals.** Voĭtovetskiĭ and co-workers[31, 34] observed for the first time the suppression of inelastic nuclear-reaction channels in diffraction of radiation by Sn^{119} in single crystals of tin (Fig. 12). The suppression effect appears in the difference of the energy dependences of the intensity of the radiation diffracted in the crystal and transmitted through the crystal off the Bragg condition. For example, in the immediate vicinity of the exact resonance, as a result of the strong absorption, no energy dependence is observed in the transmission spectrum (curve 2), i.e., total absorption of resonance γ rays is observed. For the diffracted beam in the same energy interval this dependence is clearly expressed (curve 1), i.e., total absorption is not achieved. In Fig. 12 we have indicated also the regions in which the different mechanisms of suppression of nuclear absorption are realized: 1) The region near resonance, in which nuclear scattering and absorption exceeds the scattering and absorption by electrons ($f_n > f_e$, $\mu_n > \mu_e$). Here the suppression mechanism is due mainly to interaction of γ rays with nuclei. 2) Regions in which the nuclear scattering amplitude is less than the amplitude for scattering by electrons, and the nuclear absorption is still greater than the electronic absorption ($f_n < f_e$; $\mu_n > \mu_e$). Here the suppression mechanism is due substantially to electron scattering, since in this case the formation in the crystal of a field configuration for which nuclear absorption is decreased is accomplished mainly as the result of scattering by electrons. 3) Regions in which nuclear and Rayleigh scattering are of the same order ($f_n \sim f_e$, $\mu_n > \mu_e$). Here both of the designated mechanisms are present. The asymmetry of curve 1 and the displacement of the minimum from the exact resonance are due to interference of nuclear and Rayleigh scattering. Voĭtovetskiĭ et al.[35] observed a dependence, due to dynamic effects, of the energy shape of the scattered-radiation line on the degree of perfection and the thickness of the samples.

Sklyarevskiĭ's group[36-39, 51-53, 83-87] has used 14.4-keV radiation from the isotope Fe^{57} for study of Mössbauer diffraction, employing perfect iron single crystals unenriched and enriched in the isotope Fe^{57} with a 3% addition of silicon, and single crystals of hematite and sodium nitroprusside.

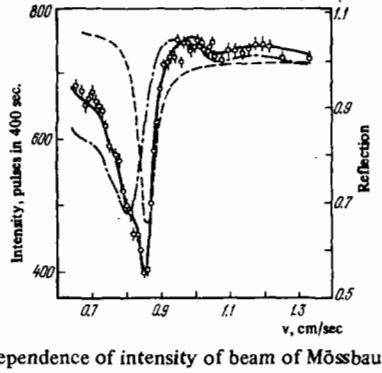

FIG. 13. Dependence of intensity of beam of Mössbauer γ rays diffracted in a single crystal of hematite, as a function of the source velocity. [38]

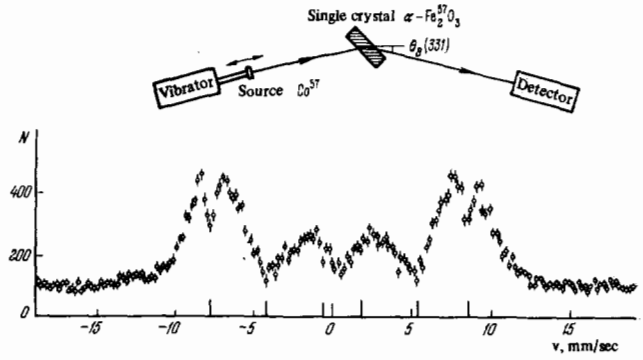

FIG. 14. Suppression effect under conditions of pure nuclear Laue reflection in an enriched single crystal of hematite. [39] The intensity of the radiation transmitted through the crystal N increases in regions of source velocities v corresponding to minima in the absorption spectrum.

Using a two-crystal diffractometer which provided high angular resolution (7″), Sklyarevskiĭ and his co-workers observed the suppression of nuclear reactions[37] in an unenriched single crystal of Fe + 3% Si. In a hematite crystal enriched to 85% Fe^{57} the suppression effect was observed, and also the nuclear Pendellosung effect (beating of the intensity of the radiation transmitted through the crystal as a function of the γ-ray energy (Fig. 13)).[38] The use of hematite (an antiferromagnetic compound) permitted Sklyarevskiĭ's group to observe dynamic effects due to pure nuclear scattering, by investigation of the magnetic diffraction peaks. Thus, they observe[53] a broadening and change in shape of the resonance line in Bragg scattering. Experiments in enriched hematite in the Laue geometry have demonstrated the suppression effect under conditions of pure nuclear scattering[39] (Fig. 14). The energy width of the scattering line measured experimentally in this work increased to 45 natural Mössbauer line widths.

c) **Diffraction in magnetically ordered crystals and crystals with a complex electric field gradient structure.** A qualitative difference of Mössbauer diffraction from x-ray diffraction involving the dependence of the resonance scattering amplitude on the magnetic field direction at the nucleus was demonstrated by Smirnov et al.[51] In this study magnetic diffraction peaks were observed for the first time in scattering in an enriched single crystal of hematite (Fig. 15). The results of the study showed that, like neutron scattering, Mössbauer diffraction can in principle be used to determine the magnetic structure of crystals. Another qualitative difference between Mössbauer diffraction and diffraction of other types of radiation, involving the dependence of the resonance scattering amplitude on the electric field gradient in the nucleus, has been demonstrated.[52, 86, 88] Mirzababaev et al.[52, 86] observed for the first time quadrupole diffraction peaks due to the existence of two different orientations of the principal axes of the electric field gradient tensor in iron nuclei located in crystallographically equivalent sites in a crystal of sodium nitroprusside. In one of these studies[88] a change in the intensity of the quadrupole reflection was observed on rotation of the crystal around a normal to the scattering plane, due to the dependence of the resonance scattering amplitude on the orientation of the principal axes of the electric field gradient tensor. Kuz'man and co-workers[89, 90], who began their diffraction studies with the familiar isotopes Sn^{119} and Fe^{57}, then carried out diffraction experiments utilizing 35.5-keV radiation of the isotope Te^{125}, in which quadrupole diffraction peaks were observed in

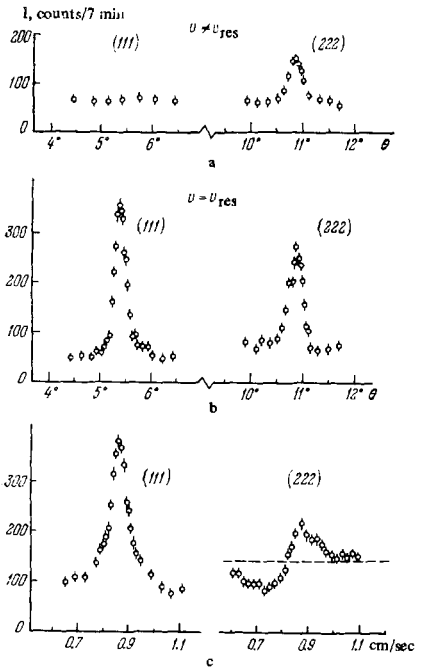

FIG. 15

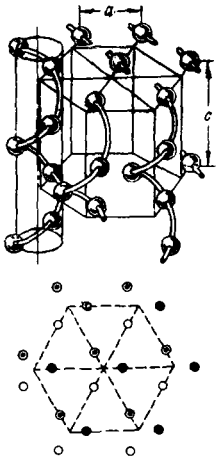

FIG. 16

FIG. 15. Magnetic diffraction peak in Bragg scattering by enriched single crystal of hematite. [51] The peak is observed when resonance scattering occurs (b) and when it is absent if there is no nuclear scattering (a). The curves of Fig. c) show the energy dependence of the scattering intensity in the magnetic (111) and crystalline (222) peaks.

FIG. 16. Structure of tellurium unit cell. In projection of the unit cell on a plane perpendicular to the C axis, we have used different designations for crystallographically equivalent sites, corresponding to the three different orientations of the principal axes of the electric field gradient tensor at these sites. [88]

scattering in tellurium single crystals.[88] The existence of quadrupole diffraction peaks for tellurium is due to the fact that in its unit cell there are three different orientations of the principal axes of the tensor of the electric field gradient in Te nuclei occupying crystallographically equivalent sites (Fig. 16). The investigations in refs. 52, 86, and 88 were carried out in compounds with a known electric field gradient structure. Their results show the possibility of obtaining information on the spatial orientation of electric field gradients in crystals by means of Mössbauer diffraction experiments.

d) Determination of the phase of the structure factor. The suggestion of using Mössbauer diffraction to determine the phase of the x-ray structure factor was made by a number of authors after publication of the first article[3] demonstrating coherence of nuclear resonance and Rayleigh scattering of γ rays. However, only two articles[14, 15] have been devoted to the experimental solution of this problem so far. Parak et al.[14] published the results of preliminary experiments and the necessary numerical calculations for determination of the structure factor phase in myoglobin. A further article[15] was devoted to a Mössbauer diffraction determination of the phase of the structure factor in the compound $K_3Fe(CN)_6$. The principle of determination of the structure factor phase is illustrated in Fig. 3. Using a single crystal of $K_3Fe(CN)_6$ enriched to 90% in the isotope Fe^{57}, these authors experimentally determined the structure factor phases of the (020) and (040) reflections. The phase values found agree with their exact values (the structure of $K_3Fe(CN)_6$ is known). Note that in determining the phase from the results of the measurements in refs. 14 and 15, the relations of the kinematic theory were used. The expressions for determination of the phase, taking into account dynamic effects, and also hyperfine splitting of the Mössbauer line, are given in refs. 91 and 92. Andreeva et al.[93] discuss the possibility of finding the phase not from the energy dependence of the nuclear amplitude, but from its dependence on the orientation of the hyperfine fields, which appears in the experiment in a change of the intensity of the reflection on rotation of the crystal around a normal to the reflecting plane (see ref. 86).

These studies[14, 15] give an idea of the laborious nature of a Mössbauer determination of the structure factor phase in a complex compound and of the requirements imposed on the experimental apparatus. The main problem which arises in Mössbauer determination of the structure factor phase is the long duration of the experiment, due to the low activity of existing Mössbauer sources. For example, in the experiment with $K_3Fe(CN)_6$ the measurement time to obtain the data for only one reflection was about a month. While noting this, Parak et al.[15] nevertheless conclude that it is possible to determine the structure factor phase experimentally by means of Mössbauer diffraction with accuracy sufficient for crystallographic determination of the structure.

e) Separation of elastic coherent and thermal diffuse scattering. The unique energy resolution of the Mössbauer effect (for example, $\sim 10^{-8}$ eV for the isotope Fe^{57}) has been used by a number of workers[94-100] to separate elastic and thermal diffuse scattering of γ rays in crystals not containing Mössbauer nuclei. Thermal diffuse scattering is accompanied by a characteristic change in the γ-ray energy by an amount of the order of 10^{-2}–10^{-3} eV. This small change in γ-ray energy for a γ-ray energy of the order of 10^4 eV cannot be observed by means of the usual x-ray technique. As a result, the information obtained by the Mössbauer method on inelastic diffuse scattering is particularly valuable. As is well known, an energy analysis of thermal diffuse scattering can be carried out by means of inelastic neutron scattering. However, the energy resolution of this method[100] (10^{-5} eV) is much poorer than that provided by the Mössbauer effect.

O'Connor and colleagues[94-96] have investigated thermal and elastic scattering and its temperature and angular dependence in the region of angles near the Bragg reflections in single crystals of lithium fluoride, barium titanate, aluminum, and potassium chloride. As a result the inelastic scattering of γ rays by optical phonons in barium titanate was observed near the phase-transition temperature. For potassium chloride and aluminum the Debye temperature was determined. The results of the Mössbauer determination of this quantity are interesting in that the Debye temperature determined from x-ray diffraction measurements contains a systematic error due to the impossibility of separating pure elastic scattering by this method.

Merlini and co-workers[97-100] have made similar studies in single crystals of silicon, aluminum, potassium chloride, and the alloy Zr-20% Nb. In these studies it was shown, in particular, that the temperature dependence of diffuse scattering observed in KCl in high orders of reflections cannot be explained just by single-phonon scattering. Account of multiphoton scattering leads to agreement of the theoretical and experimental values. Batterman et al.[100] carried out for the first time the separation of elastic and diffuse scattering in

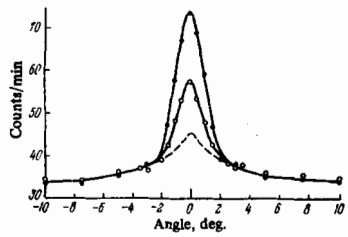

FIG. 17

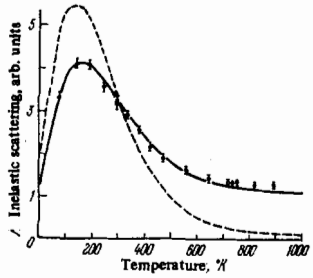

FIG. 18

FIG. 17. Angular dependence of intensity of scattering of Mössbauer radiation with energy 14.4 keV from a silicon single crystal near the (444) reflection. [97] The upper curve is the total scattering intensity, the middle curve is the result of measurements with the presence of a resonance absorber in front of the scattered γ-ray detector, and the lower curve (the dashed curve) was obtained from the first two and represents the intensity of inelastic scattering of γ rays.

FIG. 18. Temperature dependence of inelastic scattering of Mössbauer radiation with energy 14.4 keV for the (1000) reflection from a KCl single crystal. [99] The experimental results agree with the theoretical curve (solid line) obtained with inclusion of both single-phonon and multiphonon inelastic scattering. The dashed theoretical curve takes into account only single-phonon scattering.

Zr-20% Nb for scattering angles far from the Bragg peaks. These authors[100] associate the existence of a diffuse-scattering peak in the middle of the Brillouin zone with instability of the alloy studied by them with respect to a structural transition, and note the importance of the information obtained for clarifying the dynamics of this instability. Typical results of the experimental measurements are shown in Fig. 17 and 18.

f) The Mössbauer source problem. The basic scheme of experiments on Mössbauer diffraction is completely similar to that of the corresponding x-ray experiments. The difference is only that, instead of an x-ray tube, a Mössbauer source is used, and also that because of the need of making an energy analysis of the scattered radiation, a resonance absorber is placed between the detector and scatterer (Fig. 19). A quantitative difference, which grows into a qualitative difference, is the low activity of Mössbauer radiation sources existing at the present time in comparison with x-ray tubes. For a source activity of several tens of millicuries a typical value of the counting rate of scattered radiation is of the order of ten per minute. As a result, in experiments on Mössbauer diffraction, diffractometers are used which permit measurements to be made both with the Mössbauer source and an x-ray tube.[101] The use of an x-ray tube permits a substantial speedup in the adjustment of the crystal and the performance of auxiliary measurements. In addition to the low activity of Mössbauer sources, a factor which hinders the extensive use of Mössbauer diffraction in physical and applied studies is the decrease of the activity of these sources with time. For example, the half-life of an Fe^{57} Mössbauer source is 270 days, for Sn^{119} 245 days, and for Te^{125} 57 days. For this reason searches are being carried on for means of increasing the activity both of existing types of Mössbauer sources and for new principles for producing Mössbauer sources.

We will mention below two basic possibilities of producing Mössbauer sources for diffraction studies which do not decay with time. One of these is based on separation from the spectrum of an x-ray tube of radiation in a narrow energy interval and smaller solid angle,[102]

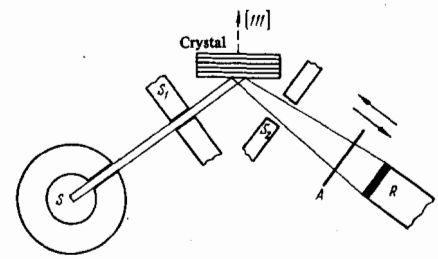

FIG. 19. Basic diagram of Mössbauer diffraction experiment. S—Mössbauer source, S_1, S_2—collimators, A—resonance absorber, R—scattered radiation detector.

and the other on use of coherent Coulomb excitation of Mössbauer nuclei[103-106] Separation of a γ-ray beam narrowly directed in space and with an energy width equal to the width of the Mössbauer transition is possible in diffraction of radiation from an x-ray tube by a crystal containing Mössbauer nuclei placed in a location corresponding to pure nuclear Bragg peaks. Here only those photons will undergo diffraction which interact resonantly with nuclei, i.e., in an energy interval determined by the width of the Mössbauer transition. However, the spectral densities of radiation of x-ray tubes existing at the present time turn out to be still insufficient for use of this means of producing a Mössbauer source.

Mössbauer γ rays emitted coherently after Coulomb excitation in a single crystal have a sharply anisotropic angular distribution.[103, 106] The allowed direction of coherent radiation is related to the crystal orientation by an expression completely similar to the Bragg condition, $\mathbf{k}_p - \mathbf{k} = \tau$, where $\mathbf{k}$ is the wave vector of the emitted γ ray, $\tau/2\pi$ is the reciprocal lattice vector of the crystal, and $k_p = (E_\gamma/\hbar v)v/v$. Here E_γ is the Mössbauer transition energy and v is the velocity of the charged particle exciting the Mössbauer level. The ratio of intensity of the coherent radiation concentrated in the small solid angle to the total radiation cross section due to the Coulomb excitation depends strongly on the particle velocity, increasing as the velocity increases, and in the limit of ultrarelativistic particles it is equal to the following product of two Lamb-Mössbauer factors, $Ce^{-2W(k)}e^{-2W(k_p)}$. (The factor C, which depends on the characteristics of the nuclear transition, is of the order of unity.) Thus, the cross section for the coherent process can be comparable with the total cross section if the probability of the Mössbauer effect in the crystal considered is sufficiently high. As is well known,[107] incoherent Coulomb excitation is used to produce Mössbauer sources and is accomplished by means of nonrelativistic particles (protons, helium ions, and so forth). In view of the fact that for an appreciable coherent excitation cross section it is necessary to use relativistic particles, in this case fast electrons are most appropriate for this purpose.[106]

6. CONCLUSION

Theoretical and experimental studies carried out up to the present time permit definite conclusions to be drawn as to the promise of further development of Mössbauer diffraction, its applications, the advances made, and also the problems which arise. In regard to applications in the field of crystal structure analysis, it can be stated on the basis of the studies made that Mössbauer diffraction (Mössbauerography) can be considered as a method supplementing the traditional diffraction methods of investigation (x-ray diffraction, neutron diffraction, electron diffraction). The selectivity of the

method, which in some cases appears as an advantage, limits the possibility of use of Mössbauerography only to objects containing Mössbauer nuclei. Thus, in problems of investigating the crystalline and magnetic structures and the structure of the electric field gradient in crystals, the application of Mössbauerography is limited to structures containing the familiar Mössbauer isotopes. In regard to investigations of the dynamics of the crystal lattice, there is no similar limitation of the objects of study, and the method itself is particularly promising in investigation of phase transformations and their dynamics.[100]

The value of theoretical studies carried out in connection with Mössbauer experiments extends beyond the field of Mössbauer diffraction and has general physical interest. Studies on the basis of the dynamical theory of interaction of resonance radiation with crystals, in particular, under conditions of hyperfine splitting of the Mössbauer line, have permitted not only description of the specific properties of Mössbauer diffraction, but also have led to a number of results applicable to description of the dynamical interaction with matter of radiations of other types, in particular neutrons[23] and visible light[108]. For example, a similar method has been successful in describing the specific optical properties of cholesteric liquid crystals.[108]

We note that interesting questions of solid-state physics on collective nuclear excitation and on the effect of the regular crystal structure on the characteristics of low-lying nuclear levels have been discussed in detail so far only theoretically (see for example refs. 25 and 109) and are awaiting experimental study. The polarization characteristics of Mössbauer scattering have not yet been studied experimentally. Nevertheless, the polarization characteristics contain information, for example, on the magnetic structure of the unit cell, and also (if hyperfine splitting of the Mössbauer line occurs in magnetically ordered crystals) can be used to determine the phase of the x-ray structure factor. The question of the effect of the crystal lattice on the angular and other characteristics of the radiation emitted by a nucleus located in a perfect crystal also awaits experimental study, although the theory of this process[110-113] has been developed in some detail.

The experimental achievement of Mössbauer diffraction is as a whole still a rather complicated matter, and therefore for the most part those experimental studies are being carried out which answer questions of a fundamental nature. The extensive introduction of Mössbauerography into the practice of applied research is limited mainly by the activity of existing Mössbauer sources. Increase of the activity of existing sources by even one order of magnitude would mean a decrease in the measurement time sufficient that the duration of the experiment would no longer be the main argument against carrying out some investigation. Therefore, the rate of penetration of Mössbauerography into applied research depends mainly on progress in perfection of Mössbauer radiation sources.

[1]H. Frauenfelder, The Mössbauer Effect, New York, W. A. Benjamin 1963. Russ. transl., IIL, 1964.
[2]Khimicheskie primeneniya mëssbauerovskoĭ spektroskopii (Chemical Applications of Mössbauer Spectroscopy) Edited by V. I. Gol'danskiĭ et al., Moscow, Mir, 1970.
[3]P. J. Black and P. B. Moon, Nature 188, 481 (1960).
[4]P. J. Black, D. E. Evans, and D. A. O'Connor, Proc R. Soc. A270, 168 (1962).
[5]P. B. Moon, Proc. R. Soc. A270, 168 (1962).
[6]C. Tzara, J. Phys. et Radium 22, 303 (1961).
[7]H. J. Lipkin, Phys. Rev. 123, 62 (1961).
[8]S. Bernstein and E. Campbell, Phys. Rev. 132, 1625 (1963).
[9]G. T. Trammell, in Chemical Effects of Nuclear Transformations, v. 1, IAEA, Vienna, 1961, p. 75.
[10]R. S. Raghavan, Proc. Ind. Ac. Sci. 53, 265 (1961).
[11]P. J. Black, Nature 206, 1223 (1965).
[12]R. N. Kuz'min, A. V. Kolpakov, and G. S. Zhdanov, Kristallografiya 11, 511 (1966) [Sov. Phys. Crystallogr. 11, 457 (1967)].
[13]G. S. Zhdanov and R. N. Kuz'min, Acta Crystallogr. B24, 10 (1968).
[14]F. Parak, R. L. Mössbauer, and W. Hoppe, Ber. Bunsenges. Phys. Chem. 74, 1207 (1970).
[15]F. Parak, R. L. Mössbauer, and U. Biebl, et al. Z. Phys. 244, 456 (1971).
[16]P. J. Black, G. Longworth, and D. A. O'Connor, Proc. Phys. Soc. Lond. 83, 925 (1964).
[17]P. J. Black, G. Longworth, and D. A. O'Connor, Proc. Phys. Soc. Lond. 83, 937 (1964).
[18]P. J. Black and J. P. Duerdoth, Proc. Phys. Soc. Lond. 84, 169 (1964).
[19]P. J. Black and J. P. Duerdoth, Acta Crystallogr. A21, pt. 17 (Suppl.), 214 (1966).
[20]D. A. O'Connor and P. J. Black, Proc. Phys. Soc. Lond. 83, 941 (1964).
[21]M. K. F. Wong, Proc. Phys. Soc. Lond. 85, 723 (1965).
[22]A. M. Afanas'ev and Yu. Kagan, Zh. Éksp. Teor. Fiz. 48, 327 (1965) [Sov. Phys. JETP 21, 215 (1965)].
[23]Yu. Kagan and A. M. Afanas'ev, Zh. Éksp. Teor. Fiz. 49, 1504 (1965) [Sov. Phys. JETP 22, 1032 (1966)].
[24]Yu. Kagan and A. M. Afanas'ev, Zh. Éksp. Teor. Fiz. 50, 271 (1966) [Sov. Phys. JETP 23, 178 (1966)].
[25]A. M. Afanas'ev and Yu. Kagan, Zh. Éksp. Teor. Fiz. 52, 191 (1967) [Sov. Phys. JETP 25, 124 (1967)].
[26]Yu. Kagan, A. M. Afanas'ev, and I. P. Perstnev, Zh. Éksp. Teor. Fiz. 54, 1530 (1968) [Sov. Phys. JETP 27, 819 (1968)].
[27]D. A. O'Connor, Proc. Phys. Soc. Lond. C1, 973 (1968).
[28]J. P. Hannon and G. T. Trammell, Phys. Rev. 169, 315 (1968).
[29]J. P. Hannon and G. T. Trammell, Phys. Rev. 186, 306 (1969).
[30]V. K. Voĭtovetskiĭ, I. L. Korsunskiĭ, and Yu. F. Pazhin, ZhÉTF Pis. Red. 8, 563 (1968) [JETP Lett. 8,343 (1968)]; Dokl. Akad. Nauk 183, 1045 (1968) [Sov. Phys. Doklady 13, 1228 (1969)].
[31]V. K. Voĭtovetskiĭ, I. L. Korsunskiĭ, and Yu. F. Pazhin, ZhÉTF Pis. Red. 8, 611 (1968) [JETP Lett. 8, 376 (1968)].
[32]V. K. Voĭtovetskiĭ, I. L. Korsunskiĭ, A. I. Novikov, and Yu. F. Pazhin, Zh. Éksp. Teor. Fiz. 54, 1361 (1968) [Sov. Phys. JETP 27, 729 (1968)].
[33]V. K. Voĭtovetskiĭ, I. L. Korsunskiĭ, A. I. Novikov, and Yu. F. Pazhin, Phys. Lett. A27, 244 (1968).
[34]V. K. Voĭtovetskiĭ, I. L. Korsunskiĭ, A. I. Novikov, and Yu. F. Pazhin, ZhÉTF Pis. Red. 11, 149 (1970) [JETP Lett. 11, 91 (1970)].
[35]V. K. Voĭtovetskiĭ, I. L. Korsunskiĭ, Yu. F. Pazhkin, and R. S. Silakov, ZhÉTF Pis. Red. 12, 314 (1970) [JETP Lett. 12, 212 (1970)].
[36]V. V. Sklyarevskiĭ, G. V. Smirnov, A. N. Artem'ev, B. Sestak, and S. Kadeckova, ZhÉTF Pis. Red. 8, 295 (1968) [JETP Lett. 8, 181 (1968)].
[37]V. V. Sklyarevskiĭ, G. V. Smirnov, A. N. Artem'ev,

R. M. Mirzababaev, B. Sestak, and S. Kadeckova, ZhÉTF Pis. Red. 11, 531 (1970) [JETP Lett. 11, 363 (1970)].
[38]G. V. Smirnov, V. V. Sklyarevskiĭ, and A. N. Artem'ev, ZhÉTF Pis. Red. 11, 579 (1970) [JETP Lett. 11, 400 (1970)].
[39]A. N. Artem'ev, R. M. Mirzababaev, V. V. Sklyarevskiĭ, G. V. Smirnov, and E. P. Stepanov, Zh. Éksp. Teor. Fiz. 64, 934 (1973) [Sov. Phys. JETP 37, 474 (1973)].
[40]Yu. Kagan and A. M. Afanas'ev, in Mössbauer Spectroscopy and Its Applications, IAEA, Vienna, 1972, p. 143.
[41]G. T. Trammell, Phys. Rev. 126, 1045 (1962).
[42]Yu. M. Aĭvazyan and V. A. Belyakov, Zh. Éksp. Teor. Fiz. 56, 346 (1969) [Sov. Phys. JETP 29, 191 (1969)].
[43]M. A. Andreeva and R. N. Kuz'min, Dokl. Akad. Nauk SSSR 185, 1282 (1969) [Sov. Phys. Doklady 14, 298 (1969)]
[44]M. A. Andreeva and R. N. Kuz'min, Kristallografiya 14, 708 (1969) [Sov. Phys. Crystallogr. 14, 605 (1969)].
[45]V. A. Belyakov and Yu. M. Aĭvazyan, Usp. Fiz. Nauk 97, 743 (1969) [Sov. Phys. Uspekhi 12, 302 (1969)].
[46]V. A. Belyakov and Yu. M. Aĭvazian, Phys. Rev. B1, 1903 (1970).
[47]V. A. Belyakov and Yu. M. Aĭvazyan, ZhÉTF Pis. Red. 7, 477 (1968) [JETP Lett. 7, 368 (1968)].
[48]V. A. Belyakov and Yu. M. Aĭvazyan, ZhÉTF Pis. Red. 9, 637 (1969) [JETP Lett. 9, 393 (1969)].
[49]A. G. Grigoryan and V. A. Belyakov, Vestn. Moskovsk. un-ta, ser. III (Fizika Astronomiya) 12 (6), 668 (1971) [Moscow University Physics Bulletin].
[50]V. A. Belyakov and R. Ch. Bokun, Izv. AN SSSR, Ser. fiz. 36, 1476 (1972) [Bull. USSR Acad. Sci., Phys. Ser., p. 1309].
[51]G. V. Smirnov, V. V. Sklyarevskiĭ, R. A. Voskanyan, and A. N. Artem'ev, ZhÉTF Pis. Red. 9, 123 (1969) [JETP Lett. 9, 70 (1969)].
[52]R. M. Mirzababaev, G. V. Smirnov, V. V. Sklyarevskiĭ, A. N. Artemev, A. N. Izrailenko, and A. V. Bobkov, Phys. Lett. A37, 441 (1971).
[53]G. V. Smirnov, V. V. Sklyarevskiĭ, A. N. Artem'ev, and R. A. Voskanyan, Phys. Lett. A32, 532 (1970).
[54]P. Imbert, Phys. Lett. 8, 95 (1964).
[55]P. Imbert, J. Phys. 27, 429 (1966).
[56]M. Blume and O. C. Kistner, Phys. Rev. 171, 417 (1968).
[57]R. W. Grant, R. M. Housley, and U. Gonser, Phys. Rev. 178, 523 (1969).
[58]Yu. M. Aĭvazyan and V. A. Belyakov, Fiz. Tverd. Tela 13, 968 (1971) [Sov. Phys. Solid State 13, 808 (1971)].
[59]V. G. Labushkin, S. N. Ivanov, and G. V. Chechin, ZhÉTF Pis. Red. 20, 349 (1974) [JETP Lett. 20, 157 (1974)].
[60]Pham Zuy Hien, Zh. Éksp. Teor. Fiz. 61,359 (1971) [Sov. Phys. JETP 34, 191 (1972)].
[61]R. M. Housley, R. W. Grant, and U. Gonser, Phys. Rev. 178, 514 (1969).
[62]F. E. Wagener, Z. Phys. 210, 361 (1968).
[63]V. B. Berestetskiĭ, E. M. Lifshitz, and L. P. Pitaevskiĭ, Kvantovaya mekhanika, ch. I, Relyativistskaya kvantovaya teoriya (Quantum Mechanics, Part I, Relativistic Quantum Theory), Moscow, Nauka, 1968.
[64]Alpha, Beta, and Gamma Spectroscopy, edited by K. Siegbahn, Amsterdam, North-Holland, 1965, Russ. Transl., Atomizdat, 1969, chapter 15.
[65]V. A. Belyakova, Zh. Éksp. Teor. Fiz. 54, 1162 (1968) [Sov. Phys. JETP 27, 622 (1963)].
[66]V. A. Belyakov and V. P. Orlov, Zh. Éksp. Teor. Fiz 56, 1366 (1969) [Sov. Phys. JETP 29, 733 (1969)].
[67]M. K. F. Wong, Phys. Rev. 149, 378 (1966).
[68]V. A. Belyakov, in Proc. of the 12th Intern. Conf. on Low Temperature Physics, Kyoto, Japan, 1970, p. 717.
[69]M. A. Poraĭ-Koshitz, Prakticheskiĭ kurs rentgenostrukturnogo analiza (Practical Course of X-Ray Structural Analysis), Moscow, Moscow University, 1960.
[70]D. T. Keating, Phys. Rev. 178, 732 (1969).
[71]M. A. Andreeva and R. N. Kuz'min, Kristallografiya 18, 407 (1973) [Sov. Phys. Crystallogr. 18, 645 (1973)].
[72]Pham Zuy Hien, Zh. Éksp. Teor. Fiz. 59, 2083 (1970) [Sov. Phys. JETP 32, 1130 (1971)].
[73]I. P. Perstnev and F. N. Chukhovskiĭ, Fiz. Tverd. Tela 16, 3011 (1974) [Sov. Phys. Solid State 16, 1946 (1975)].
[74]M. A. Andreeva and R. N. Kuz'min, Kristallografiya 19, 1002 (1974) [Sov. Phys. Crystallogr. 19, 620 (1974)]; M. A. Andreeva and R. N. Kuz'min, Vestn. Moskovsk. un-ta, ser. III (Fizika, Astronomiya) 15 (2), 178 (1974) [Moscow University Physics Bulletin].
[75]V. A. Belyakov, Fiz. Tverd. Tela 13, 3320 (1971) [Sov. Phys. Solid State 13, 2789 (1971)].
[76]B. W. Batterman and H. Cole, Rev. Mod. Phys. 36, 681 (1964).
[77]W. H. Zachariasen, X-Ray Diffraction in Crystals, N.Y. – L., Wiley and Sons, 1946.
[78]V. A. Belyakov, Fiz. Tverd. Tela 13, 2170 (1971) [Sov. Phys. Solid State 13, 1824 (1971)].
[79]A. M. Afanas'ev and Yu. Kagan, Zh. Éksp. Teor. Fiz. 64, 1958 (1973) [Sov. Phys. JETP 37, 987 (1973)].
[80]Yu. Kagan and A. M. Afanas'ev, Z. Naturforsch A28, 1351 (1973).
[81]A. M. Afanas'ev and I. P. Perstnev, Zh. Éksp. Teor. Fiz. 65, 1271 (1973) [Sov. Phys. JETP 38, 630 (1974)].
[82]V. A. Belyakov and E. V. Smirnov, Zh. Éksp. Teor. Fiz. 68, 608 (1975) [Sov. Phys. JETP 41, No. 2 (1975)].
[83]A. N. Artem'ev, V. V. Sklyarevskiĭ, G. V. Smirnov, and E. P. Stepanov, ZhÉTF Pis. Red. 15, 320 (1972) [JETP Lett. 15, 226 (1972)].
[84]A. N. Artem'ev, I. P. Perstnev, V. V. Sklyarevskiĭ, G. V. Smirnov, and E. P. Stepanov, Zh. Éksp. Teor. Fiz. 64, 261 (1973) [Sov. Phys. JETP 37, 136 (1973)].
[85]E. P. Stepanov, A. N. Artem'ev, I. P. Perstnev, V. V. Sklyarevskiĭ, and G. V. Smirnov, Zh. Éksp. Teor. Fiz. 66, 1150 (1974) [Sov. Phys. JETP 39, 562 (1974)].
[86]R. M. Mirzababaev, V. V. Sklyarevskiĭ, and G. V. Smirnov, Phys. Lett. A41, 349 (1972).
[87]A. N. Artem'ev, V. V. Sklyarevskiĭ, G. V. Smirnov, and E. P. Stepanov, Zh. Éksp. Teor. Fiz. 63, 1390 (1972) [Sov. Phys. JETP 36, 736 (1973)].
[88]V. S. Zasimov, R. N. Kuz'min, A. Yu. Aleksandrov, and A. I. Firov, ZhÉTF Pis. Red. 15, 394 (1972) [JETP Lett. 15, 277 (1972)].
[89]V. S. Zasimov, R. A. Kuz'min, and A. I. Firov, Vestn. Moskovsk. un-ta, ser. III (Fizika. Astronomiya) 12 (3), 324 (1971) [Moscow University Physics Bulletin].
[90]V. S. Zasimov, R. N. Kuz'min, and A. I. Firov, Kristallografiya 17, 864 (1972) [Sov. Phys. Crystallogr. 17, 757 (1972)].
[91]F. N. Chukhovskiĭ and I. P. Perstnev, Acta Cryst. A28, 467 (1972).
[92]I. P. Perstnev and F. N. Chukhovskiĭ, Kristallografiya 18, 926 (1973) [Sov. Phys. Crystallogr. 18, 582 (1973)].
[93]M. A. Andreeva, R. N. Kuzmin, and S. Oparina, Phys. Status Solidi d63, K147 (1974).
[94]D. A. O'Connor and N. M. Butt, Phys. Lett. 7, 233 (1963).
[95]N. M. Butt and D. A. O'Connor, Proc. Phys. Soc. Lond. 90, 247 (1967).
[96]D. A. O'Connor and E. R. Spicer, Phys. Lett. A29, 136 (1969).
[97]G. Ghezzi, A. Merlini, and S. Pace, Nuovo Cimento 64B, 103 (1969).

[98]G. Albanese, C. Ghezzi, A. Merlini, and S. Pace, Phys. Rev. **B5**, 1746 (1972).
[99]G. Albanese, C. Ghezzi, and A. Merlini, Phys. Rev. **B7**, 65 (1973).
[100]B. W. Batterman, G. Maracci, A. Merlini, and S. Pace, Phys. Rev. Lett. 31, 227 (1973).
[101]A. N. Artem'ev, K. P. Aleshin, R. M. Mirzababaev, V. V. Sklyarevskiĭ, and E. P. Stepanov, Prib. Tekh. Éksp., No. 6, 64 (1971) [Instrum. Exper. Tech.].
[102]R. N. Kuz'min, A. V. Kolpakov, and G. E. Zhdanov, Vestn. Moskovsk. un-ta, ser. III (Fizika. Astronomiya) **10** (3), 99 (1969) [Moscow University Physics Bulletin].
[103]Yu. M. Kagan and F. N. Chukhovskiĭ, ZhÉTF Pis. Red. 5, 166 (1967) [JETP Lett. 5, 133 (1967)].
[104]É. A. Perel'shteĭn and M. I. Podgoretskiĭ, Yad. Fiz. **12**, 1149 (1970) [Sov. J. Nucl. Phys. **12**, 631 (1971)].
[105]A. V. Kolpakov, Yad. Fiz. **16**, 1003 (1972) [Sov. J. Nucl. Phys. 16, 554 (1973)].
[106]V. A. Belyakov and V. P. Orlov, Phys. Lett. A44, 463 (1973).
[107]Effekt Mëssbauera (The Mössbauer Effect), Moscow, Atomizdat, 1969.
[108]V. A. Belyakov and V. E. Dmitrienko, Fiz. Tverd. Tela. 15, 2724 (1973) [Sov. Phys. Solid State 15, 1811 (1973)].
[109]P. A. Aleksandrov, Zh. Éksp. Teor. Fiz. 65, 2047 (1973) [Sov. Phys. JETP **38**, 1022 (1974)].
[110]P. A. Aleksandrov and Yu. Kagan. Zh. Éksp. Teor. Fiz. **59**, 1733 (1970) [Sov. Phys. JETP **32**, 942 (1971)].
[111]P. A. Aleksandrov, Zh. Éksp. Teor. Fiz. 67, 728 (1974) [Sov. Phys. JETP **40**, No. 2 (1975)].
[112]J. P. Hannon, N. J. Carron, and G. T. Trammell, Phys. Rev. **B9**, 2810 (1974).
[113]J. P. Hannon, N. J. Carron, and G. T. Trammell, Phys. Rev. **B9**, 2791 (1974).
[114]Z. G. Pinsker, Dinamicheskoe rasseyanie rentgenskikh lucheĭ v ideal'nykh kristallakh (Dynamic Scattering of X Rays in Ideal Crystals), Moscow, Nauka, 1974.

Translated by C. S. Robinson